Investigation of Factors Affecting the Gaseous and Particulate Matter Emissions from Diesel Vehicles

Bei Wang[1*], Yik-Sze Lau[2], Yuhan Huang[3], Bruce Organ[3,4], Shun-Cheng Lee[5], Kin-Fai Ho[2*]

[1] Faculty of Science and Technology, Technological and Higher Education Institute of Hong Kong, Hong Kong

[2] School of Public Health and Primary Care, The Chinese University of Hong Kong, Hong Kong

[3] Centre for Green Technology, School of Civil and Environmental Engineer, University of Technology Sydney, NSW 2007, Australia

[4] Jockey Club Heavy Vehicle Emissions Testing and Research Centre, Hong Kong

[5] Department of Civil and Structural Engineering, The Hong Kong Polytechnic University, Hong Kong

Abstract

The current study presents a detailed investigation of diesel vehicle emissions utilizing chassis dynamometer testing. Nitrogen oxides (NO_x), total hydrocarbon (THC), carbon monoxide (CO), and particulate matter (PM) were chosen to be the targets of this study. The recruited vehicle fleet consists of 15 in-use diesel vehicles, spanning a wide range of emission standards, engine sizes, weight, model year, etc. The real-time measurement data collected in different tests, as well as the mass of PM collected on filters, are used to calculate the emission factors (*EF*) of vehicles under various driving conditions. Results show that in general, *EFs* of NO_x, CO, THC, and PM of the recruited fleet span a wide range of value (NO_x: 0.80 ± 0.34 g kg^{-1} to 60.28 ± 2.94 g kg^{-1}; THC: 0.10 ± 0.04 g kg^{-1} to 5.28 ± 1.28 g kg^{-1}; CO: below detection limits to 24.01 ± 8.48 g kg^{-1}; PM: below detection limits to 2.47 ± 1.22 g kg^{-1}). Further data analysis shows that the implementation of a higher emission standard has a significant effect on reducing the emission of pollutants, except for NO_x. Driving conditions are also the important factors affecting the *EFs* of target pollutants. Besides, statistical analysis shows a significant correlation between *EFs* of NO_x with the testing weight and the maximum engine power of the vehicle. Further investigation is recommended to explore the effect of maintenance of the vehicles to the vehicular emission.

Keywords: Diesel engine; Criteria air pollutants; Emission factor; Emission standard.

[*] Corresponding authors. E-mail address: beiwang@vtc.edu.hk; kfho@cuhk.edu.hk

INTRODUCTION

In Hong Kong, the number of motor vehicles has kept increasing throughout the last few decades. According to the Transport Department, there were 766,200 licensed vehicles running on the road by the end of 2017, which was increased by 26% compared to 2010 (Hong Kong Transport Department, 2017). Since vehicle exhaust is considered to be the largest single source of pollution in urban area (Mayer, 1999), the continuously expanding fleet produces serious air pollution problems in Hong Kong.

Criteria air pollutants refer to six pollutants commonly found in ambient air, which were first introduced by the United States Environmental Protection Agency (USEPA). They are ground-level ozone (O_3), carbon monoxide (CO), nitrogen dioxides (NO_2), sulphur dioxide (SO_2), lead (Pb) and particulate matter (PM). Various studies have shown that the elevated level of criteria air pollutants was associated with different levels of adverse health effects, including asthma (Curtis et al., 2006; Delfino et al., 2003; Lee et al., 2002), respiratory tract infections (Salvi et al., 1999), allergic rhinitis (Wang et al., 2015), ischaemic heart disease (Sydbom et al., 2001), lung cancer and cardiopulmonary mortality (Pope III et al., 2002). On the other hand, CO_2 is regarded as the most important greenhouse gas (GHG), which causes global warming owing to its high value of radiative forcing (Forster et al., 2007). The transport sector is one of the main sources of CO_2 emissions, which is responsible for a quarter of global energy related CO_2 emissions. Other major CO_2 emission sectors include industry (37%), residential (22%) and commerce and public

services (8%) (IEA, 2017). In addition, road transport is the only sector with increasing CO_2 emissions due to economic and population growth (European Commission, 2019; Huang et al., 2019c). The 2017 International Energy Agency (IEA) data showed that the energy use in transport significantly increased from 23% of total final consumption in 1971 to 29% in 2015. To combat climate change and to achieve a sustainable low carbon future, a landmark agreement – the Paris Agreement – was reached on 12 December 2015, which on average required most countries to reduce their CO_2 emissions by 33% in 2030 compared to 2005 levels (Huang et al., 2018a). To achieve this abatement target, the road transport sector must make a significant contribution, considering the fact that transport is the only major sector with increasing CO_2 emissions. Although diesel vehicles are more efficient than gasoline vehicles (emitting less CO_2 on a g/kW-h basis) and there are more gasoline vehicles, diesel vehicles usually have larger engines and are used much more intensively (e.g. public buses and goods vehicles) than gasoline vehicles (e.g. private cars). Consequently, the total amount of energy consumed by diesel vehicles is also significant. The US Energy Information Administration (EIA) reported that the global market shares of gasoline and diesel fuels were 39% and 36% in 2012, respectively, and both would have the same market share of 33% in 2040 (EIA, 2019).

The Hong Kong Government has set up a detailed guideline on the level of criteria pollutants and other harmful substances to control the local air quality, known as the Air Pollution Control

Ordinance. These pollutants are monitored by 16 air quality monitoring stations located in different districts in Hong Kong. According to the Hong Kong Environmental Protection Department (HKEPD, 2017), levels of air pollutants have been significantly reduced in the last two decades. For example, from 1997 to 2015 the annual average concentrations of SO_2, NO_x, respirable suspended particulates (RSP) and CO have decreased by 76%, 40%, 69%, and 45% respectively (HKEPD, 2017). It is worth mentioning that NO_x and CO showed the least reductions. This was because ambient CO concentration was generally very low and thus a further significant reduction should not be expected. In 2018, the maximum hourly CO value was 2.61 mg m^{-3} and the maximum daily CO average was 2.05 mg m^{-3} in Hong Kong, which were well within the AQO limits of 30 mg m^{-3} for 1-hour value and 10 mg m^{-3} for 8-hour average (HKEPD, 2019). On the other hand, NO_x was a pollutant that has yet achieved the AQO limits (HKEPD, 2019) and the lower reduction rate would be caused by the following two factors. Firstly, diesel NO_x emissions were not decreasing with European automotive emission standards as expected (Carslaw et al., 2011; 2013; Huang et al. 2018b). Secondly, the real-driving NO_x emissions of diesel vehicles were significantly higher than the laboratory test results and type-approval limits (Degraeuwe and Weiss, 2017; Kousoulidou et al., 2013; Weiss et al., 2011).

The Hong Kong Government has also launched several programs to reduce the problem of street-level air pollution. These programs include the promotion of electric vehicles, tax

incentives for environment-friendly private cars and commercial vehicles, the promotion of the use of biodiesel, low emission zones, and gasoline and LPG high-emitters enforcement by on-road remote sensing technology. In addition, the Hong Kong government has employed the European Emission Standard since 1992, which serves as the main driving force for reducing vehicle emissions. The increasingly stringent emission standard triggered the development of emission control measures, such as the installation of after-treatment devices and the use of unleaded and low sulphur content fuels. It should be noted that air quality in some districts in Hong Kong still fails to meet the requirements set by the government with all these vehicle emission controlling measures implemented. For example, NO_2 concentrations in Hong Kong downtown areas, such as Causeway Bay, Central, and Mongkok, exceeded both the 1-hour Air Quality Objective (AQO) of 200 μg m^{-3} and the annual AQO of 40 μg m^{-3} (HKEPD, 2018).

In the recent decades, diesel vehicle has gained more and more attention because of its increasing popularity in the European market and other places in the world. As at end April 2019, there were 149,158 registered diesel vehicles in Hong Kong, which was increased by 3% compared to the number of registered diesel vehicles in 2013 (Hong Kong Transport Department, 2019). The advantages of diesel vehicle include lower price, higher power output, and higher fuel economy compared to its gasoline counterpart. However, it should be noted that diesel vehicles are the primary source of street-level pollution in Hong Kong (Lee et al., 2006). According to the

Hong Kong Environment Bureau (2013), although there were only about 88,000 pre-Euro IV diesel commercial vehicles running on road, they accounted for about 88% of RSP and 46% NO_x emission of the whole vehicular fleet in Hong Kong. Diesel vehicles are reported to be the major source of air pollution in terms of NO_x and PM emissions, but emit less CO, HC and CO_2 emissions than gasoline vehicles. Although diesel vehicles only represent a relatively small share (~10%) of the global on-road vehicles, they produce significant percentages (70%-90%) of the total NO_x and PM emissions (Anenberg et al., 2017; Huang et al., 2019a; Liu et al., 2018). These NO_x and PM emissions are the biggest concerns due to their adverse effects on environment and public health and are the main air pollution problems in Hong Kong, as well as many other megacities worldwide. On the other hand, both gasoline and diesel vehicles are relatively clean in CO and HC emissions which are usually well complied with the automotive emission standards (Huang et al., 2019b; Kousoulidou et al., 2013; Weiss et al., 2011) and the air quality objectives (HKEPD, 2018).

This study aims to investigate the emissions of THC, NOx, CO and PM from different diesel vehicles under different driving conditions. Recruited vehicles were tested on chassis dynamometer equipped in a certified vehicle testing laboratory. To the best of our knowledge, previous studies of diesel vehicle emissions in Hong Kong were mainly carried out by tunnel measurement, vehicle plume chasing or on-road remote sensing (Chan and Ning, 2005; Chan et

al., 2007; Ho et al., 2009; Lau et al., 2015; Ning et al., 2012). Although there are many published studies on diesel vehicle emissions using chassis dynamometers, these studies usually tested only one or a few vehicles, such as: Li et al. (2013) tested one light-duty gasoline vehicle; Liu et al. (2017) tested two gasoline passenger cars; Jung et al. (2017) tested three diesel passenger cars; Nakashima and Kajii (2017) tested six gasoline passenger cars; Louis et al. (2016) tested six Euro 4-5 gasoline and diesel passenger cars. There were a few studies in which more vehicles were tested, while these usually only studied limited emission species or vehicle types, such as: Huang et al. (2017) evaluated emissions of 51 Euro 2-5 light-duty gasoline vehicles; Pang et al. (2014) investigated VOCs of 1612 light-duty gasoline vehicles; Huang et al. (2019b) tested gaseous emissions of 183 diesel vans. One of the main contributions of this study is that it investigated the emission characteristics of 15 in-use diesel vehicles, covering a wide range of emission standards (from Euro 2 to 6), vehicle types (from passenger cars of 2.2 t to heavy goods vehicles up to 23 t), mileage (from 5883 to 440048 km), and exhaust after-treatment technologies (from vehicles with no after-treatment to those with EGR, DOC, SCR and DPF). The investigated emissions included both gaseous and PM emissions. In addition, four test conditions, including cold-start, hot-start, idling and steady-state cycles, were tested and compared in this study. The results and conclusions obtained in this study are applicable to both Hong Kong and other cities.

METHODS

145 ***Fleet overview and instrumentation***

146 The tested diesel vehicles in this study were selected to cover a wide range of model years,
147 engine sizes, after-treatment technologies, and emission standards. Based on these criteria, 15
148 diesel vehicles were recruited, and their specifications are listed in Table 1. All of the tested
149 diesel vehicles were from Asian manufacturers since the Asian manufacturers dominated the
150 market share of diesel vehicles in Hong Kong. A recent study showed that the Hong Kong diesel
151 vehicle fleet was dominated by only seven models, accounting for 78% of the total real-world
152 vehicle use (Huang et al., 2018c). These manufactures are Toyota, Hyundai, Isuzu and Nissan.
153 The tested vehicles were categorized regarding to the United Nations Economic Commission for
154 Europe (UNECE) categories (UNECE, 2011a). Passenger cars (PCs) are vehicles defined as M
155 type in UNECE categories. Light-duty vehicles (LDVs), medium-duty vehicles (MDVs) and
156 heavy-duty vehicles (HDVs) correspond to N1, N2, and N3 type vehicles in UNECE categories,
157 respectively. The only exception is Vehicle 15, which is a 10-ton tractor categorized as HDV in
158 this study. Since Vehicle 15 is designed to carry trailer up to 20 tons, it is reasonable to put it into
159 the HDV category.

160 The diesel vehicles were tested on chassis dynamometers in the Jockey Club Heavy Vehicle
161 Emissions Testing and Research Centre (JCEC) in Hong Kong. Fig. 1 shows a schematic diagram
162 of the instrumental setup. All testing instruments in JCEC comply with the European standards

for type approval tests. Two chassis dynamometers designed for vehicles of different weight were used in this study. For PCs and LDVs, testing was performed on a Mustang Dynamometer with 48" single roller; while for MDVs and HDVs, a Mustang Dynamometer with 17.2" triple roller was used. SIGNAL instruments were used to monitor and record the instantaneous concentrations of the gaseous pollutants with a frequency of 1 Hz. THC and NO_x were measured using heat flame ionization (FID) (Signal Model 3000HM THC Analyzer) and chemiluminescent detectors (Signal Model 4000VM NO_x Analyzer), respectively. For CO and CO_2, non-dispersive infrared detectors (Signal Model 7100M CO IRGA Analyzer, Signal Model 7200M CO_2 IRGA Analyzer) were used. PM samples were collected on Teflon membrane filters (Pall, 47 mm) over the whole driving cycle for the calculation of PM mass emission. The weight of Teflon filter was measured before and after sample collection by a microbalance (Sartorius, MC5) with readability of 0.001 mg. Filters were conditioned in a humidity-controlled chamber (relative humidity = 40%) for at least 24 hours before weighing.

Driving Cycles

Different driving cycles were used to simulate different driving conditions in the real world. In the current study, four driving cycles were tested for each tested vehicle. They are the cold-start transient cycle, hot-start transient cycle, idling cycle, and steady-state cycle. For simplicity, cold-start and hot-start transient cycles will be called cold-start and hot-start cycles hereafter. For each

vehicle, three replicates of hot-start, idling, and steady-state cycles and two replicates of cold-start cycle were performed.

The cold-start and hot-start cycles used in the current study combine different driving scenarios, such as urban, rural, and highway driving, to simulate real-world driving conditions. They share the same driving pattern but different starting conditions. For a cold-start cycle, the vehicle was soaked in ambient condition overnight before testing, which represents an engine starts at cold condition. For a hot-start cycle, the engine of the vehicle was warmed-up by previous tests before starting the cycle. Cold-start and hot-start cycles were tested because engine start had significant effect on the overall cycle performance, especially the cold start due to the higher friction losses, lower thermal efficiency, and incomplete combustion (Zare et al, 2017; 2018).

Two different transient cycles were used for vehicles of different categories. New European Driving Cycle (NEDC), which has been used for the type-approval test of European Emission Standard, was utilized for testing LDVs and PCs. On the other hand, type approval tests for European Emission Standard for MDVs and HDVs are carried out by an engine dynamometer using the European Transient Cycle (ETC) rather than a chassis dynamometer. Therefore, to comply with the requirement of the current study, FIGE (Forschungsinstitut für Geräusche und Erschütterungen) cycle, which is the chassis dynamometer version of ETC, was used for the testing of MDVs and HDVs. The driving patterns of the two transient cycles are shown in Fig. 2.

To assess the emissions of vehicles during idling and constant speed driving conditions, idling and steady-state cycles were used. Idling and steady-state tests are simple, fast and cost-effective methods to evaluate the performance of a vehicle. Such cycles are highly simplified cycles, compared with real-world driving (e.g. portable emission measurement system (PEMS) test) and type approval test cycles (e.g. NEDC and FTP). For an idling cycle, the vehicle was parked on the chassis dynamometer and switched on the engine only during the sample collection. For a steady-state cycle, the measurement was performed when the vehicle was running at 50 km h^{-1} constantly. 50 km h^{-1} was chosen because the speed limit of most of the roads in Hong Kong (except highways) is 50 km h^{-1}. The duration of both cycles were 20 minutes.

A loading factor was added to the vehicles when they were running on the chassis dynamometer. For PCs, LDVs and MDVs, 50% loading was added to simulate their normal working condition. The loading factor was added to the vehicles by increasing the roller resistance of the dynamometer dynamically.

For HDVs, the loading value was different from the rest of the fleet. Preliminary tests showed that Vehicle 14 could not complete the whole FIGE cycle with 50% loading due to the meltdown of the tire at the high-speed driving part of the cycle. The problem arose from the accumulation of heat generated between the roller and the tire during the prolonged high-speed driving. Besides, the second half of the FIGE cycle has a maximum speed over 70 km h^{-1}, which exceeds the

legally permitted speed of HDVs in Hong Kong. Therefore, for Vehicle 14, loading was set to 10% and the maximum speed was reduced to 57 km h^{-1}. For Vehicle 15, which is a 10-ton tractor, loading of the dynamometer was set to 23 tons in order to simulate the condition of pulling a trailer. For the sake of consistency, the FIGE cycle run by Vehicle 15 is the same as Vehicle 14 (i.e. maximum speed reduced).

Calculation of emission factors

The concentration of each gaseous pollutant was measured on-line throughout the whole test. The total amount of a gaseous pollutant emitted over the whole driving cycle can be calculated by Equation (1)

$$M_p = \sum_{i=1}^{t} C_{pi} V_i \qquad (1)$$

where,

M_p: Mass of gaseous pollutant p in [g]

C_{pi}: Background corrected concentration of pollutant p at i^{th} second in [g m^{-3}]

V_i: Volume flow of diluted exhaust through the CVS system at i^{th} second in [m^3]

t: Time duration of the test in [s]

For the calculation of PM mass emitted from the whole driving cycle, the weight of sample collected on the Teflon filter is used. The average mass concentration of PM of diluted exhaust

passed through the filter can be calculated from the mass of sample on the Teflon filter and the total volume flow of diluted exhaust through the filter by the following equation:

$$C_{PM} = \frac{M_{TF}}{V_{TF}} \qquad (2)$$

where:

C_{PM}: Average mass concentration of PM of diluted exhaust in each trial of test in [g L^{-1}]

M_{TF}: Mass of PM collected on Teflon filter in [g]

V_{TF}: Total volume flow of diluted exhaust through the Teflon filter in [L]

Since C_{PM} also represents the average mass concentration of PM in the dilution tunnel for the whole trial, the mass of PM emitted from the vehicle can be directly calculated by multiplying C_{PM} by the total volume of diluted exhaust passed through the dilution tunnel.

$$M_{PM} = C_{PM} \times V_{total} \qquad (3)$$

where:

M_{PM}: Mass of PM emitted from the vehicle in each trial of the test in [g]

V_{total}: Total volume flow of diluted exhaust through the dilution tunnel in each trial of the test in [L]

The total amount of pollutant (M_p and M_{PM}) can be used to calculate the *EF* of the vehicle. A commonly employed *EF* is the amount of pollutant emitted per kilometer travelled by the vehicle. However, the distance specific *EF* cannot be used to compare the idling result with other testing

252 results since the vehicle is not running during the idling cycle. Therefore, a fuel-based *EF*
253 approach is used in this study. The fuel-based *EF* is defined as the amount of pollutant emitted
254 per kilogram of fuel consumed by the vehicle (Kirchstetter et al., 1999; Miguel et al., 1998). The
255 value of fuel consumption can be derived from the mass emission of CO_2. Due to the high
256 combustion efficiency of diesel engines, it is reasonable to assume that CO_2 is the major
257 combustion product while the contribution of other carbon containing species is negligible (Ning
258 et al., 2008; Yli-Tuomi et al., 2005). Therefore, the fuel consumption of the vehicle in a testing
259 cycle can be calculated by a simple carbon mass balance approach given by Equation (4)

260 $$\frac{V_f \times \varrho_f \times \omega_f}{MW_C} = \frac{M_{CO_2}}{MW_{CO_2}} \qquad (4)$$

261 where,

262 V_f: Volume of fuel consumed in [L]

263 ϱ_f: Density of diesel fuel in [kg L^{-1}]

264 ω_f: Mass fraction of carbon in diesel fuel

265 M_{CO_2}: Background corrected mass of CO_2 produced in a test cycle in [g]

266 MW_C: Molecular mass of carbon in [g mol^{-1}]

267 MW_{CO_2}: Molecular mass of CO_2 in [g mol^{-1}]

268 Equation (4) is based on the fact that 1 mole of carbon atom in fuel produces 1 mole of CO_2. ϱ_f
269 is taken to be 0.832 kg L^{-1} while ω_f is taken to be 0.87 from other studies (Kirchstetter et al.,

1999; Yli-Tuomi et al., 2005). The *EF* in gram per kilogram of fuel consumed (g kg^{-1}) can be calculated by Equation (5) after obtaining the fuel consumption V_f from equation (4)

$$EF = \frac{M_{p/PM}}{V_f \times \varrho_f} \qquad (5)$$

For the calculation of *EF* of NO_x, the effects of ambient humidity and temperature need to be considered (Lindhjem et al., 2004; Yanowitz et al., 2000). The calculation of humidity correction factor k_h in this study is following the UNECE standard described in UNECE (2011b). All NO_x data presented in this paper is humidity corrected by k_h given by Equation (6)

$$k_h = \frac{1}{1 - 0.0329(H - 10.71)} \qquad (6)$$

in which:

$$H = \frac{6.211 \times R_a \times P_d}{P_B - P_d \times R_a \times 10^{-2}}$$

Where:

H: Absolute humidity expressed in grams of water per kilogram of dry air

R_a: Relative humidity of the ambient air expressed as a percentage

P_d: Saturation vapor pressure at the ambient temperature in [kPa]

P_B: Atmospheric pressure in the test cell in [kPa]

RESULTS AND DISCUSSION

General overview

288 *EFs* of CO, THC, NO_x, and PM of the 15 tested vehicles under different driving conditions are
289 summarized in Fig. 3. In general, *EFs* of all pollutants span a wide range of value. *EF*s of NO_x
290 range from 0.80 ± 0.34 g kg^{-1} (Vehicle 7, steady-state) to 60.28 ± 2.94 g kg^{-1} (Vehicle 15,
291 steady-state). For THC, the lowest *EF* is 0.10± 0.04 g kg^{-1} in hot-start test of Vehicle 7 while the
292 highest one is 5.28±1.28 g kg^{-1} in idling test of Vehicle 8. In the case of CO, the lowest *EF* is
293 found in the steady-state test of Vehicle 2, which is below the detection limits. The highest *EF* of
294 CO is found in the idling test of Vehicle 9 with a value of 24.01 ± 8.48 g kg^{-1}. *EFs* of PM also
295 vary among tested vehicles. The *EF* of PM is below the detection limits in the hot-start test of
296 Vehicle 2 while the highest value is up to 2.47±1.22 g kg^{-1} in hot-start test of Vehicle 15.
297 Fig. 3 also shows that diesel vehicles are relatively clean in CO and THC emissions regardless
298 of the driving cycle or vehicle age, but are high in NO_x emissions. This is mainly because diesel
299 engines (also usually referred as compression ignition engines) are operated under lean
300 combustion conditions (diffusion/non-premixed flames) which have low CO and HC emissions
301 but are prone to produce NO_x and PM emissions. HC, CO and NO_x have different/conflicting
302 emission formation mechanisms where HC and CO are results of unburnt and incomplete
303 combustion respectively (mainly rich fuel combustion) while NO is formed in high-temperature
304 rich-oxygen condition (slightly lean fuel combustion). Such results in Fig. 3 agree well with
305 previous vehicle emission studies using plume chasing and remote sensing. Lau et al. (2015)

collected a large amount of on-road vehicle emission data of Hong Kong highways used plume chasing method. The results showed that not all high-emitters are from those vehicles of older Euro standards, and high-emitters for one pollutant may not be a high-emitter for another pollutant. Huang et al. (2018d) evaluated the emissions performance of diesel vehicles in Hong Kong using on-road remote sensing technology. The results showed that high-emitters had little overlapping between CO, HC and NO, particularly NO was involved.

CO, THC, and NO_x would react with other chemical components in the atmosphere to induce the formation of ozone. The diesel vehicular emission ratios of these gaseous pollutants are informative with regard to potential impacts on ozone formation and helpful to refine the air quality models. The mass ratios of CO/NO_x and THC/NO_x from 15 diesel vehicles are shown in Fig. 4. The average CO/NO_x mass ratios are 0.516 for cold-start transient cycle, 0.317 for hot-start transient cycle, 0.570 for idling, and 0.396 for steady-state, respectively. Rappengluck et al. (2013) reported the CO/NOx ratio of 0.42 for heavy-duty diesel vehicles by using Motor Vehicle Emission Simulator, which is very close to the values obtained in this study. In general, the ratios of THC/NO_x are higher in the idling and steady-state cycles than the cold-start and hot-start transient cycles. The average THC/NO_x ratios are 0.063 for cold-start transient cycle, 0.062 for hot-start transient cycle, 0.125 for idling, and 0.118 for steady-state, respectively. The average mass ratios of THC/NO_x are the lowest for HDVs, followed by PCs. Bishop et al. (2012)

measured on-road light-duty vehicle emissions in California by remote sensing testing, and reported the average HC/NO_x mass ratio of 0.6, which is higher than the value obtained in this study. The reason of higher mass ratio of HC/NO_x is that the gasoline vehicles were the major tested vehicles and the diesel vehicles only accounted for about 1.3% of the measurements in their study.

For gaseous pollutants, idling cycles usually produce the highest *EFs*, followed by transient cycles. In the case of PM, transient cycles produce higher *EFs* than steady-state and idling cycles. The dashed line in Fig. 3 shows the average *EF* over all driving cycles (i.e. cold-start, hot-start, idle, and steady-state) for each tested vehicle. In the following sections, factors affecting the emission pattern of the pollutants are discussed in detail.

Driving conditions

Gaseous pollutants

Four driving conditions are tested for each vehicle (cold-start, hot-start, idling and steady-state) on the chassis dynamometer. In order to study the effect of driving conditions on pollutant emission, *EFs* of the same vehicle class (i.e. PC, LDV, MDV, and HDV) and same driving condition are averaged for a given pollutant, and the results are shown in Fig. 5.

341 A striking feature of Fig. 5 is that among the four driving conditions, the idling cycle always
342 produces the highest *EFs* in gaseous pollutants (except NO_x emission in HDVs). In the idling
343 cycle test, the vehicle was mounted on the dynamometer with only the engine on. Other
344 accessory loadings, such as air-conditioning and headlights, were switched off. The excess
345 emission of THC and CO during the idling cycle could be explained by the incomplete
346 combustion of fuel. In idling condition, the engine cannot work at its optimum temperature, and
347 thus the combustion process is "less complete" compared to transient and steady-state conditions
348 (Rahman et al., 2013). Since THC and CO are mainly derived from the incomplete combustion of
349 fuel in the engine, it is very likely that vehicles in the idling cycle produce more THC and CO
350 than in other driving modes. In the case of NO_x, the excess emission in the idling cycle probably
351 comes from the lower Exhaust Gas Recirculation (EGR) efficiency or the stop of operation of the
352 EGR system. Some engine manufacturers may use auxiliary emission control devices which will
353 shut off the EGR valve after the engine has been run on idling condition for a certain period to
354 prevent the fouling of the EGR and engine intake system (Khan et al., 2006). For vehicles
355 without an EGR system (Vehicle 1 and 3), the observed high NO_x emission is probably caused by
356 the poor atomization of fuel and working condition of the engine in low temperature.
357 The average THC *EFs* in the steady-state and transient cycles are low and have similar values.
358 Low THC emission is an intrinsic advantage of diesel engines over their gasoline counterparts

359 due to the air rich (fuel lean) combustion condition. Although a vehicle will consume more fuel
360 and emit more THC in a hot-start cycle than in a steady-state cycle, the effect will be eliminated
361 by the fuel-based *EF* calculation approach (Yanowitz et al., 1999; Yao et al., 2015). It is expected
362 that the *EF* of THC would be higher in cold-start condition due to the "less complete"
363 combustion condition at low engine temperature. However, the above feature is not observed in
364 Fig. 5 because THC emissions from the tested vehicles are so low that any instrumental noise
365 signals would probably mask the slight difference between the cold-start and hot-start cycles.
366 A similar trend is observed for CO emissions, where vehicles in steady-state and hot-start
367 cycles have similar CO emissions. However, unlike THC, CO emissions in cold-start cycle show
368 an observable elevation compared to hot-start cycle. This observation arises from the poor
369 combustion condition during cold-start and warm-up phases of the engine which facilitates the
370 formation of the incomplete combustion product. The difference between cold-start and hot-start
371 is more significant in PC and LDV categories than in MDV and HDV categories. The reason is
372 some of the tested vehicles in PC and LDV categories emit much more CO in the cold-start cycle
373 (e.g. Vehicle 4 and 6) than in the hot-start cycle, which drags up the average value in cold-start
374 CO emission.
375 The main difference between NO_x and the other two gaseous pollutants is their formation
376 mechanism in diesel engines. CO and THC are mainly derived from the incomplete combustion

377 of fuel, and therefore their emissions are relatively low due to the lean combustion condition in
378 diesel engines. On the other hand, NO_x is formed in the engine by completely different
379 mechanism. In general, there are two widely accepted formation pathways of NO_x in diesel
380 engines. The first one is called thermal (Zeldo'vich) mechanism and NO_x produced by this
381 pathway is called thermal NO_x. Thermal NO_x is formed through the dissociation of molecular
382 nitrogen and oxygen. Since the activation energy of this reaction is high, the formation of thermal
383 NO_x is favored at high temperature (above 1900 K) and oxygen-rich condition (Musculus, 2004).
384 The second mechanism involves the reaction between hydrocarbon radicals and molecular
385 nitrogen forming amines or cyano intermediates which subsequently react to give NO_x (Miller
386 and Bowman, 1989). NO_x produced by this mechanism is called prompt NO_x, and it is mainly
387 formed in fuel rich condition.
388 Referring to Fig. 5, NO_x emissions from MDVs and HDVs in cold-start cycles are higher than
389 in hot-start cycles. This trend can also be observed in most of the vehicles in these two categories
390 as shown in Fig. 3. However, excess NO_x in cold-start transient cycle has not been widely
391 reported. Armas et al. (2012) reported a higher NO_x emission when the engine started at a cold
392 condition and stated that the observation could be explained by the delay of EGR valve opening
393 in the cold-start condition. However, delayed EGR valve opening should not be the main reason
394 in the case of the current study because delayed EGR valve opening only happens in the very

395 early part of the cycle and therefore contributes very little to the overall emission in the whole
396 cycle. Weilenmann et al. (2005) observed an increase in NO_x with decreasing ambient
397 temperature and Tang et al., (2008) found NO_x emission in cold-start condition was 1.4 times
398 higher than in hot-start condition. However, both studies did not propose any explanations for the
399 observation. Higher NO_x emission in cold-start condition may be caused by the enriched engine
400 operation condition and the higher combustion temperature (Bielaczyc et al., 2001). During the
401 cold-start and warm-up phases, more-than-usual fuel is injected into the combustion chamber to
402 help for the start-up of the engine since the atomization and vaporization of fuel is poor in low
403 temperature. The enriched mixture of fuel and air increases the combustion temperature and
404 therefore favors the formation of thermal NO_x. At the same time, the production rate of prompt
405 NO_x may also increase since the mixture is more fuel-rich. The combination of the two
406 circumstances may account for the observed elevation of NO_x in cold-start condition. Dardiotis et
407 al. (2013) compared emission of NO_x in cold-start conditions at 22 ˚C and -7 ˚C and reported that
408 the reason for the higher NO_x emission might come from the lower EGR rate at -7˚C, which was
409 to prevent the formation of condensation products in the EGR line. This reason may also
410 contribute to the observation of higher NO_x in cold-start cycles in this study, but it fails to
411 account for the higher NO_x emission in tested vehicles without an EGR system (Vehicle 1 and 3).

412 For PCs and LDVs, the average NO_x *EFs* for cold-start and hot-start cycles are very similar,
413 with the hot-start cycle having a little bit higher *EFs*. The difference in emission compared to
414 MDVs and HDVs mainly comes from the difference in the transient cycle used. As mentioned in
415 the methodology part, FIGE cycle was used for MDVs and HDVs while NEDC cycle was used
416 for PCs and LDVs. In order to illustrate the effect of different driving cycles on NO_x emission, a
417 cumulative curve of average NO_x concentration is plotted (Fig. 6). Since the concentration of NO_x
418 was measured every second during vehicle testing, an average NO_x concentration of each second
419 can be obtained by averaging the NO_x concentrations of all vehicles using the same driving cycle
420 in the same second. Then the average NO_x concentration of each second is used to construct a
421 cumulative curve of concentration of NO_x throughout the whole cycle, as shown in Fig. 6. It can
422 be seen that for FIGE cycle NO_x emission is higher in cold-start cycle than in hot-start cycle. For
423 NEDC, NO_x emissions are very similar in hot-start and cold-start cycles. The difference between
424 cold-start and hot-start FIGE cycle is more significant than NEDC cycle because the first part of
425 FIGE cycle involves rigorous accelerations and decelerations (as shown in the speed trace in Fig.
426 6(b)) which leads to the production of more NO_x. The high NO_x production rate exaggerates the
427 difference between cold-start and hot-start conditions. For vehicles running NEDC cycle, NO_x
428 emissions in cold-start and hot-start condition are almost the same throughout the whole cycle.
429 This observation may be attributed to the less demanding operation condition of NEDC compared

to FIGE cycle. As shown in Fig. 6(a), in the first 780 seconds (urban driving cycle section) of NEDC, both acceleration and deceleration patterns are smooth and regular. Under the above condition, NO_x emission is low, and thus the difference between cold-start and hot-start is not significant. More NO_x is produced in the latter part of NEDC (the extra-urban driving cycle) as suggested by the steeper slope of the cumulative emission curve in Fig. 6(a). However, since the engine conditions are almost the same after the first 780 seconds, the emissions are again similar for cold-start and hot-start cycles. Therefore, NO_x emissions in cold-start and hot-start NEDC cycle do not show a significant difference, and this gives rise to the observation in Fig. 5 that vehicles running FIGE cycle have different NO_x emission characteristics compared to vehicles running NEDC cycle. In general, NO_x emissions in the steady-state cycle are low because constant speed cruising requires less power from the engine compared to transient cycles, and steady-state cycle is run after the engine has fully warmed up.

PM emission

PM in diesel engine exhaust is mainly derived from fuel droplet pyrolysis, unburned fuel, lubricating oil, and combustion byproducts (Shah et al., 2004). Fig. 5 shows that PM *EFs* are higher in transient cycles than in idling and steady-state cycles. This observation is consistent with other studies (Shah et al., 2004; Zheng et al., 2017). In transient driving conditions, higher fuel to air equivalence ratios are required to generate the output power for the acceleration of the

448 vehicles (Zervas and Bikas, 2008) compared to idling or steady-state conditions, which will result
449 in higher PM emissions.
450 Unlike gaseous pollutants, PM emissions from cold-start and hot-start cycles do not have a
451 significant difference. Dwyer et al. (2010) investigated the difference in PM mass emission
452 between a cold-start NEDC and a NEDC after running a pre-conditioning cycle. Their results
453 showed that the effect of cold-start condition on PM mass emission was insignificant, which
454 agreed with the result in the current study. However, Fontaras et al. (2014) reported a factor of
455 about 1.3 of cold-start excess emission of PM in the UDC part (first 780 seconds) of NEDC and
456 attributed the reason to the inefficient after-treatment device operation during the start-up of the
457 driving cycle. It should be noted that the results in the current study correspond to the PM emitted
458 from the whole NEDC, not only the UDC part of the NEDC. It is expected that the later part of
459 NEDC would emit more PM since it involves accelerations at higher speed. The hot-start PM
460 emission seems to be higher than cold-start emission in LDV. Referring to Fig. 3, the difference
461 between hot-start and cold-start PM emissions in LDV mainly arises from the results of Vehicle 6
462 and 7, of which emissions in the hot-start cycles are substantially higher than in the cold-start
463 cycles. However, it is noteworthy that the standard deviations of the results in the hot-start cycles
464 are large, which means that more samples will be needed before reaching a conclusion.
465

Emission standard

Gaseous pollutants

The effect of vehicle emission standard on gaseous pollutant and PM emissions can be assessed by the average *EFs* over all driving conditions as shown by the dashed lines in Fig. 3. For CO emission, it can be observed that the average *EFs* for PCs, LDVs and MDVs generally decrease with increasing emission standard. For example, in MDVs, the average *EFs* decrease from 12.73 ± 0.53 g kg^{-1} (Vehicle 8, Euro 3) to 3.33 ± 0.14 g kg^{-1} (Vehicle 13, Euro 5). However, Vehicle 3 and 4 (LDVs, Euro 2 and 3) do not follow this trend. One possible explanation is that the testing weight of Vehicle 4 (2265 kg) is slightly higher than Vehicle 3 (2195 kg), where the extra loading to the engine leads to a higher emission of CO in Vehicle 4. Another possible reason is that Vehicle 3 has better maintenance so that emission is lower than expected. For HDVs, CO emissions increase with increasing emission standard. Again, it is probably because the testing weight of Vehicle 15 is higher than Vehicle 14. Moreover, the emission limit of CO does not change from Euro 4 to Euro 5 for heavy-duty vehicles. Therefore, HDVs do not show a similar trend in CO emission with other vehicle classes.

For THC, the emission characteristic is similar to CO, of which the average *EFs* generally decrease with increasing emission standards. For example, the average *EFs* in MDVs decrease from 2.47 ± 0.13 g kg^{-1} (Vehicle 8, Euro 3) to 0.86 ± 0.18 g kg^{-1} (Vehicle 13, Euro 5). The

similarity shared by CO and THC comes from their common formation mechanism, which is the incomplete combustion of fuel. An exceptional case is Vehicle 2 in the PC category, which shows a higher average emission of THC compared to its Euro 3 counterpart (Vehicle 1). The higher average *EF* of THC observed in Vehicle 2 is attributed to the high THC emission in the idling cycle. The reason for this observation is unclear. Nevertheless, the values of averaged *EFs* of Vehicle 1 and 2 are very small which makes any source of instrumental error would significantly affect the results. In any case, Vehicle 2 is the only Euro 6 vehicle tested, and a more extensive study is recommended to evaluate the emission of vehicles with high emission standards.

NO_x emission shows a different scenario compared to CO and THC. In general, NO_x emission does not show any particular trend or strong correlation with emission standard. For PCs and MDVs, the average NO_x *EFs* fluctuate within a narrow range while for LDVs and HDVs, some extreme values are observed (Vehicle 5 and 15) regardless of the emission standards. The lack of trend in NO_x emission with emission standards was also reported by other studies (Huo et al., 2012; Wang et al., 2012; Yanowitz et al., 2000). Some studies pointed out that the above-mentioned phenomenon came from the manipulation of the engine performance to meet the emission requirements in type approval tests (Huo et al., 2012; Yanowitz et al., 2000), while some suggested that the discrepancy came from the ineffective operation of after-treatment devices (Weiss et al., 2012). In the case of this study, the latter reason might play a more critical

502 role. As shown in Table 1, most of the tested vehicles have very high pre-test odometer readings
503 (average value of 227872 km), which means that they have been run for a long distance or time
504 before testing. These vehicles are subjected to different levels of maintenance and therefore the
505 performance of their after-treatment devices (the main after-treatment device for NO_x is EGR in
506 this study) may vary significantly. Since NO_x emission is primarily controlled by after-treatment
507 devices, the experimental results do not show any correlation between NO_x *EFs* and vehicle sizes,
508 as well as emission standards. The drastically high *EF* of NO_x of Vehicle 15 is also probably
509 caused by the poor maintenance of the after-treatment device. Vehicle 15 is a Euro 5 HDV
510 equipped with Selective Catalytic Reduction (SCR) system, which is the leading method in NO_x
511 controlling technology (Johnson, 2014). However, it was observed that white smoke with
512 pungent ammonia smell came out from Vehicle 15 during the transient cycle testing, which was
513 very likely caused by the leakage of urea from the SCR system.

514 *PM emission*

515 The effect of emission standards on PM emission is significant. Referring to Fig. 3, a clear
516 trend of decreasing PM *EF* with increasing emission standards can be observed for LDVs and
517 MDVs. The decrease of PM emission in PC is not obvious in the figure. Two exceptional cases
518 are observed in Vehicle 6 and Vehicle 15. The reason for the exceptionally high PM emission for
519 Vehicle 6 is unclear since all parameters (e.g. mileage, testing weight and model year) are similar

520 with other vehicles in the same class. The testing weight of Vehicle 15 is 4000 kg which is higher
521 than Vehicle 14, so a higher *EF* is expected. Nevertheless, the *EF* of Vehicle 15 is too high for a
522 Euro 5 standard vehicle, and further investigation is necessary for this kind of heavy-duty tractor.
523
524 ***Comparison of NO_x and PM emission with European Emission Standards***
525 Although the emission standard assigned for a vehicle only restricts its emission after coming
526 out from the factory, it is still essential to check whether it will follow or seriously deteriorate
527 from the initial emission standard after running for a certain period of time. Among the above-
528 discussed pollutants, NO_x and PM are of higher concern in both environmental and health aspects.
529 The cold-start and steady-state emissions of NO_x and PM of all vehicles are summarized in Figs.
530 7(a) and 7(b). The black dashed lines in the figure correspond to the Euro 3 emission standard for
531 MDV. From Fig. 7(a), most of the data points are gathered at the bottom left of the graph, with
532 some extreme emitters (e.g. Vehicle 15) far above the emission limits. Another observation from
533 Fig. 7(a) is that not many vehicles exceed the limits of PM and NO_x at the same time (Vehicle 15
534 in both cycles and Vehicle 8 and 9 in cold-start cycle only). In Fig. 7(b), it is observed that most
535 of the vehicles in cold-start cycles exceed only the emission limit of NO_x. In the case of steady-
536 state cycle, half of the vehicles show NO_x emissions higher than the limit. An important message
537 obtained from Fig. 7 is that vehicles tested in the current study perform worse in NO_x emission

than in PM emission, which means that emission control by restricting the emission standard of a vehicle is less successful in NO_x. It should also be noted that the emission standard applied in Fig. 7 is for Euro 3 MDV while most of the vehicles in the current study have more advanced emission standards. However, results show that a lot of these Euro 4 and 5 vehicles cannot comply with the Euro 3 standard. Therefore, controlling emissions by improving the emission standard of the vehicle alone may not be enough, especially for NO_x. Long-term monitoring campaign and more frequent maintenance are required to bring the emission of pollutants to a desired level.

Testing Weight, Mileage and Maximum engine power

Besides emission standard, vehicle class, driving mode, and other vehicle characteristics may also influence the emission of a vehicle. In the following part, testing weight (inertial weight of the vehicle plus a loading factor), mileage (pre-test odometer reading), and maximum engine power (MEP) of the vehicle will be investigated for their correlation with the emissions of the target pollutants. These parameters are chosen because they reflect different areas that may affect the emission of a vehicle. Testing weight affects the loading of the engine, mileage reflects the general condition of the vehicle, and maximum power controls the output energy and fuel consumption of the engine.

556 Correlations between the emission of pollutants and different parameters are evaluated by
557 multiple regression model. However, preliminary analysis shows that the testing weight and
558 maximum engine power of the vehicles in the current study exhibit multicollinearity and
559 therefore, it is not suitable to put them into the model together. Preliminary analysis on CO and
560 THC results shows that no statistically significant correlation exists between them and the three
561 parameters (testing weight, mileage, and MEP) under any driving conditions. For PM, the
562 emission is controlled mainly by after-treatment devices (e.g. whether a vehicle is equipped with
563 DPF or not would have tremendous different levels of emissions) and therefore it is hard to obtain
564 any correlations between PM emission and the three parameters. In the following discussion, the
565 focus will be put on NO_x.
566 In the previous discussion, it has been reported that driving cycle has a significant effect on the
567 emission characteristic of NO_x. Therefore, samples are divided into PC+LDV and MDV+HDV
568 since these two groups use different transient cycles in testing. Results of linear regression
569 analysis and their corresponding R^2 and p-value for NO_x are listed in Table 2. Although most of
570 the results do not show any significant correlation, surprisingly small p-value and relatively large
571 R^2 values are found in some specific combinations.
572 *Testing weight*

When the vehicles were tested on a chassis dynamometer, a corresponding loading was added on top of the inertial weight of the vehicle according to the method described in the methodology part, and the resulting value is called the testing weight of the vehicle. Testing weight is selected rather than vehicle weight because the engine and after-treatment devices may have different levels of response to the loading added. Thus, testing weight is a better representative of real-world driving conditions as vehicles are seldom driven with 0% loading. Data of the idling cycle is not analyzed in this session because the roller of the chassis is not moving during the idling cycle.

As shown in Table 2, good correlations between the testing weight of MDV + HDV and NO_x *EFs* are found under cold-start (R^2=0.81, p<0.005) and hot-start (R^2=0.67, p<0.05) conditions. Figs. 8(a) and 8(b) show the plots of NO_x *EFs* against the testing weight of the vehicle for cold-start and hot-start conditions. This finding may provide extra information to modelling studies of NO_x emission contributed by MDVs and HDVs. Also, the R^2 and p-values obtained show that the testing weight of the vehicle has a better correlation with NO_x emission in cold-start cycle than in hot-start cycle. One possible reason is that after the vehicle has warmed-up, the engine and after-treatment devices are running in an optimal condition which effectively reduces the emission of NO_x. Since the effectiveness of NO_x reduction by these devices is regardless of the testing weight,

590 the additional factor diminishes the correlation between testing weight and NO_x emission in hot-
591 start cycle.

592 Unlike MDVs and HDVs, NO_x *EFs* of PCs and LDVs do not show any significant correlation
593 with their corresponding testing weight in both cold-start and hot-start cycles. As shown in Figs.
594 8(a) and 8(b), the correlations are statistically insignificant in both cold-start (R^2=0.20, p=0.3) and
595 hot-start (R^2=0.30, p=0.2) cycles. The above observation is possibly caused by the small sample
596 size and the narrow range of testing weight (2150 to 2650 kg) of the recruited PCs and LDVs.
597 The NO_x *EFs* scatter around the best fit straight line of the data with some extremely large
598 (Vehicle 5) and small (Vehicle 2, 7) values. A larger data set is needed to get a deeper insight into
599 the correlation between NO_x emission and vehicle testing weight.

600 *Maximum engine power*

601 Since every engine has different maximum power output at a certain engine speed, the emission
602 characteristic would be different even under the same driving cycle. To simplify the analysis, the
603 MEP of the vehicle is used for the regression analysis regardless of the engine speed.

604 A correlation is found under the linear regression model between the MEP and the NO_x *EFs* in
605 MDV + HDV in both cold-start and hot-start conditions (Figs. 8(c) and 8(d)). The correlation is
606 found better in cold-start cycle (R^2=0.92, p<0.0005) than in hot-start cycle (R^2=0.77, p<0.005).
607 Compared with the results in testing weight, the correlation with MEP shows larger R^2 and

608 smaller *p*-values, which means that the MEP is a better predictor for NO_x emission than the
609 testing weight of the vehicle. For PCs and LDVs, the correlation is statistically insignificant.
610 In general, characteristics observed in the correlation between NO_x *EFs* and testing weight are
611 also observed in the correlation with MEP. The reason for this observation is that the weight of
612 the vehicle is one of the parameters governing the design of a suitable engine power. Other
613 factors affecting the MEP include the design of the engine and the purpose of the vehicle. Results
614 in this part serve as new initiatives for further study to qualify and quantify the effect of MEP on
615 NO_x emission in modelling study or environmental policy development.
616 *Mileage*
617 The mileage of the vehicles recruited spans an extensive range of value from 5883 km to
618 440048 km, with an average value of 227872 km. Vehicles with higher mileage are expected to
619 emit more pollutants since their engine conditions could be worse than vehicles with lower
620 mileage. However, as shown in Table 2 there is no statistically significant correlation between the
621 mileage of the vehicle and NO_x *EFs* in any driving conditions under the linear regression model.
622 The reason is that the sample size of this study (15 vehicles in total) is relatively small, and the
623 tested vehicles are subjected to different levels of maintenance. Moreover, some vehicles do not
624 have any after-treatment devices while others are equipped with different after-treatment devices.
625 All these factors distort the emission pattern of NO_x, and therefore no correlation can be observed.

626

627 ## CONCLUSIONS

628 Various factors are investigated for their effects on emissions of NO_x, THC, CO and PM from
629 diesel vehicles in this study. Emission standards and driving conditions of the diesel vehicles are
630 the two main factors governing the emissions of the target pollutants. In most of the cases, the
631 evolution of emission standard has a robust effect on reducing the emission of gaseous pollutants,
632 except for NO_x. On the other hand, the diesel vehicles in idling condition generate the highest
633 fuel specific emission factor in all diesel vehicle classes and all gaseous pollutants, except for
634 NO_x emission in HDV. The diesel vehicles in transient driving cycles produce the second highest
635 emission factor. Cold-start cycles produce higher emissions of pollutants than hot-start cycles in
636 most of the cases, except for NO_x in PCs and LDVs, where the emissions in hot-start cycles are
637 slightly higher than in cold-start cycles. This observation arises from the different transient
638 driving cycles used. FIGE cycle used for MDVs and HDVs involves more vigorous driving
639 condition in the start-up and warm-up states compared to the NEDC, therefore exaggerates the
640 difference in emissions between cold-start and hot-start conditions. Evolution of emission
641 standard also has a significant effect on the reduction of PM. Transient cycles produce the highest
642 *EFs* of PM, but the emission seems not to be affected by starting condition (i.e. cold-start or hot-
643 start). Comparison of PM and NO_x emission with Euro 3 emission standard for MDV shows that
644 NO_x emission deteriorates from the emission standard more than PM emission, which points out

645 that current policies and regulations in emission control could not reduce the emission of NO_x as
646 effective as PM.

647 Statistical analysis of different vehicle parameters with the *EF* of NO_x shows that there is a
648 significant correlation between NO_x *EF* and the testing weight of the diesel vehicle, as well as the
649 MEP of the diesel vehicle. The unique data set obtained in the current study can serve as a
650 reference for further modelling analysis on criteria air pollutants and policy-making processes
651 related to air pollution.

652 Last but not least, it is observed that a few diesel vehicles are emitting significant amounts of
653 pollutants despite their high emission standards (e.g. Vehicle 5 and 15). These diesel vehicles
654 usually have high odometer readings and inefficient after-treatment devices (e.g. SCR of Vehicle
655 15 was not functioning properly during testing), which all point to poor maintenance of the diesel
656 vehicles. It is expected that the maintenance of the engine and after-treatment devices plays a
657 crucial role in controlling the emission of diesel vehicles and this should be the next topic for
658 policymakers and researchers to address.

659

660 ## Acknowledgements

661 The work described in this paper was supported by a grant from the Research Grants Council
662 of the Hong Kong SAR, China (UGC/FDS25/E06/15).

663

664 **REFERENCES**

665 Anenberg, S. C., Miller, J., Minjares, R., Du, L., Henze, D. K., Lacey, F., Malley, C. S.,
666 Emberson, L., Franco, V., Klimont, Z., Heyes, C., (2017). Impacts and mitigation of excess
667 diesel-related NOx emissions in 11 major vehicle markets. *Nature.* 545: 467-471.
668 Armas, O., García-Contreras, R., Ramos, Á., (2012). Pollutant emissions from engine starting
669 with ethanol and butanol diesel blends. *Fuel Process Technol.* 100: 63-72.
670 Bielaczyc, P., Merkisz, J., Pielecha, J., (2001). Investigation of exhaust emissions from DI diesel
671 engine during cold and warm start. *SAE J-Automot Eng*, 2001-01-1260.
672 Bishop, G.A., Schuchmann, B.G., Stedman, D.H., Lawson, D.R., (2012). Multispecies remote
673 sensing measurements of vehicle emissions on Sherman Way in Van Nuys, California. *J. Air*
674 *Waste Manag. Assoc.*, 62, 1127-1133.
675 Carslaw, D. C., Beevers, S. D., Tate, J. E., Westmoreland, E. J., Williams, M. L., (2011). Recent
676 evidence concerning higher NOx emissions from passenger cars and light duty vehicles. *Atmos*
677 *Environ.* 45: 7053-7063.
678 Carslaw, D. C., Rhys-Tyler, G., (2013). New insights from comprehensive on-road measurements
679 of NOx, NO2 and NH3 from vehicle emission remote sensing in London, UK. *Atmos Environ.*
680 81: 339-347.
681 Chan, T. and Ning, Z., (2005). On-road remote sensing of diesel vehicle emissions measurement
682 and emission factors estimation in Hong Kong. *Atmos Environ*. 39(36): 6843-6856.

683 Chan, T., Ning, Z., Wang, J., Cheung, C., Leung, C., Hung, W., (2007). Gaseous and Particle
684 Emission Factors from the Selected On-Road Petrol/Gasoline, Diesel, and Liquefied Petroleum
685 Gas Vehicles. *Energ Fuel.* 21: 2710-2718.
686 Curtis, L., Rea, W., Smith-Willis, P., Fenyves, E., Pan, Y., (2006). Adverse health effects of
687 outdoor air pollutants. *Environ Int.* 32(6): 815-830.
688 Dardiotis, C., Martini, G., Marotta, A., Manfredi, U., (2013). Low-temperature cold-start gaseous
689 emissions of late technology passenger cars. *Appl Energ.* 111: 468-478.
690 Degraeuwe, B. and Weiss, M., (2017). Does the New European Driving Cycle (NEDC) really fail
691 to capture the NOX emissions of diesel cars in Europe? *Environ Pollut.* 222: 234-241.
692 Delfino, R., Gong, H., Linn, W., Pellizzari, E., Hu, Y., (2003). Asthma symptoms in hispanic
693 children and daily ambient exposures to toxic and criteria air pollutants. *Environ Health Persp.*
694 111(4): 647-656.
695 Dwyer, H., Ayala, A., Zhang, S., Collins, J., Huai, T., Herner, J. and Chau, W., (2010). A study
696 of emissions from a Euro 4 light duty diesel vehicle with the European particulate
697 measurement programme. *Atmos Environ.* 44(29): 3469-3476.
698 European Commission, 2019. A European Strategy for low-emission mobility. Available at:
699 https://ec.europa.eu/clima/policies/transport_en, (accessed July 2019).

EIA, 2019. Transportation sector energy consumption. Available at: https://www.eia.gov/outlooks/ieo/pdf/transportation.pdf, (accessed July 2019).

Fontaras, G., Franco, V., Dilara, P., Martini, G. and Manfredi, U., (2014). Development and review of Euro 5 passenger car emission factors based on experimental results over various driving cycles. *Sci Total Environ.* 468-469: 1034-1042.

Forster, P., Ramaswamy, V., Artaxo, P., Berntsen, T., Betts, R., Fahey, D.W., Haywood, J., Lean, J., Lowe, D.C., Myhre, G., Nganga, J., Prinn, R., Raga, G., Schulz, M., Van Dorland, R., (2007). Changes in atmospheric constituents and in radiative forcing. In: *Solomon, S. (Ed.), Climate Change 2007: The Physical Science Basis. Contribution of Working Group I to the Fourth Assessment Report of the Intergovernmental Panel on Climate Change.* Cambridge University Press, Cambridge, United Kingdom and New York, NY, USA.

Ho, K., Ho, S., Lee, S., Cheng, Y., Chow, J., Watson, J., Louie, P., Tian, L., (2009). Emissions of gas- and particle-phase polycyclic aromatic hydrocarbons (PAHs) in the Shing Mun Tunnel, Hong Kong. *Atmos Environ.* 43(40): 6343-6351.

Hong Kong Environment Bureau, 2013. Item for finance committee. Available at: http://www.legco.gov.hk/yr13-14/english/fc/fc/papers/f13-52e.pdf, (accessed September 2017).

Hong Kong Environmental Protection Department (HKEPD), 2017. Emission trend (1997 – 2015). Available at:

718 http://www.epd.gov.hk/epd/english/environmentinhk/air/data/emission_inve.html, (accessed
719 September 2017).
720 Hong Kong Environmental Protection Department (HKEPD), 2018. Air Quality Statistics in 2017.
721 Available at: https://www.epd.gov.hk/epd/english/environmentinhk/air/data/aq_stat.html
722 (accessed July 2019).
723 Hong Kong Environmental Protection Department (HKEPD), 2019. Air Quality Statistics.
724 Available at: https://www.epd.gov.hk/epd/english/environmentinhk/air/data/aq_stat.html,
725 (accessed July 2019).
726 Hong Kong Transport Department, 2017. The Annual Traffic Census 2017. Available at:
727 https://www.td.gov.hk/filemanager/en/content_4915/annual%20traffic%20census%202017.pdf,
728 (accessed July 2019).
729 Hong Kong Transport Department, 2019. Registration and Licensing of Vehicles by Fuel Type
730 (April 2019). Available at: https://www.td.gov.hk/filemanager/en/content_4940/table44.pdf,
731 (accessed July 2019).
732 Huang, C., Tao, S., Lou, S., Hu, Q., Wang, H., Wang, Q., Li, L., Wang, H., Liu, J. g., Quan, Y.,
733 Zhou, L., (2017). Evaluation of emission factors for light-duty gasoline vehicles based on
734 chassis dynamometer and tunnel studies in Shanghai, China. *Atmos Environ.* 169: 193-203.

735 Huang, Y., Ng, E. C. Y., Zhou, J. L., Surawski, N. C., Chan, E. F. C., Hong, G., (2018a). Eco-
736 driving technology for sustainable road transport: A review. *Renew Sustain Energy Rev.* 93:
737 596-609.
738 Huang, Y., Organ, B., Zhou, J.L., Surawski, N.C., Hong, G., Chan, E.F.C., Yam, Y.S., (2018b).
739 Remote sensing of on-road vehicle emissions: Mechanism, applications and a case study from
740 Hong Kong. *Atmos Environ.* 182: 58-74.
741 Huang, Y., Yam, Y. S., Lee, C. K. C., Organ, B., Zhou, J. L., Surawski, N. C., Chan, E. F. C.,
742 Hong, G., (2018c). Tackling nitric oxide emissions from dominant diesel vehicle models using
743 on-road remote sensing technology. *Environ Pollut.* 243: 1177-1185.
744 Huang, Y., Organ, B., Zhou, J.L., Surawski, N.C., Hong, G., Chan, E.F.C., Yam, Y.S., (2018d).
745 Emission measurement of diesel vehicles in Hong Kong through on-road remote sensing:
746 Performance review and identification of high-emitters. *Environ Pollut.* 237: 133-142.
747 Huang, Y., Ng, E.C.Y., Yam, Y.S., Lee, C.K.C., Surawski, N.C., Mok, W.C., Organ, B., Zhou,
748 J.L., Chan, E.F.C., (2019a). Impact of potential engine malfunctions on fuel consumption and
749 gaseous emissions of a Euro VI diesel truck. *Energy Convers Manage.* 184: 521-529.
750 Huang, Y., Organ, B., Zhou, J.L., Surawski, N.C., Yam, Y.S., Chan, E.F.C., (2019b).
751 Characterisation of diesel vehicle emissions and determination of remote sensing cutpoints for
752 diesel high-emitters. *Environ Pollut.* 252: 31-38.

753 Huang, Y., Surawski, N. C., Organ, B., Zhou, J. L., Tang, O. H. H., Chan, E. F. C., (2019c). Fuel
754 consumption and emissions performance under real driving: Comparison between hybrid and
755 conventional vehicles. *Sci Total Environ.* 659: 275-282.
756 Huo, H., Yao, Z., Zhang, Y., Shen, X., Zhang, Q., He, K., (2012). On-board measurements of
757 emissions from diesel trucks in five cities in China. *Atmos Environ.* 54: 159-167.
758 International Energy Agency (IEA), 2017. World energy balances: Overview. International
759 Energy Agency.
760 Johnson, T., (2014). Review of Selective Catalytic Reduction (SCR) and Related Technologies
761 for Mobile Applications. In: *Urea-SCR Technology for deNO_x After Treatment of Diesel*
762 *Exhausts*, Springer, New York.
763 Jung, S., Lim, J., Kwon, S., Jeon, S., Kim, J., Lee, J., Kim, S., (2017). Characterization of
764 particulate matter from diesel passenger cars tested on chassis dynamometers. *J Environ Sci.*
765 54: 21-32.
766 Khan, A., Clark, N., Thompson, G., Wayne, W., Gautam, M., Lyon, D., Hawelti, D., (2006). Idle
767 emissions from heavy-duty diesel vehicles: review and recent data. *JAPCA J Air Waste Ma*.
768 56(10): 1404-1419.

769 Kirchstetter, T., Harley, R., Kreisberg, N., Stolzenburg, M., Hering, S., (1999). On-road
770 measurement of fine particle and nitrogen oxide emissions from light- and heavy-duty motor
771 vehicles. *Atmos Environ.* 33(18): 2955-2968.
772 Kousoulidou, M., Fontaras, G., Ntziachristos, L., Bonnel, P., Samaras, Z., Dilara, P., (2013). Use
773 of portable emissions measurement system (PEMS) for the development and validation of
774 passenger car emission factors. *Atmos Environ.* 64: 329-338.
775 Lau, C.F., Rakowska, A., Townsend, T., Brimblecombe, P., Chan, T., Yam, Y., Močnik, G., Ning,
776 Z., (2015). Evaluation of diesel fleet emissions and control policies from plume chasing
777 measurements of on-road vehicles. *Atmos Environ.* 122: 171-182.
778 Lee, J., Kim, H., Song, H., Hong, Y., Cho, Y., Shin, S., Hyun, Y., Kim, Y., (2002). Air pollution
779 and asthma among children in Seoul, Korea. *Epidemiology.* 13(4): 481-484.
780 Lee, S.C., Cheng, Y., Ho, K.F., Cao, J.J., Louie, P.K.K., Chow, J.C., Watson, J.G., (2006).
781 PM1.0 and PM2.5 characteristics in the roadside environment of Hong Kong. *Aerosol sci Tech.*
782 40: 157-165.
783 Li, T., Chen, X., Yan, Z., (2013). Comparison of fine particles emissions of light-duty gasoline
784 vehicles from chassis dynamometer tests and on-road measurements. *Atmos Environ.* 68: 82-91.

785 Lindhjem, C., Chan, L.M., Pollack, A., (2004). Applying humidity and temperature corrections to
786 on and off-road mobile emissions. 13th International Emission Inventory Conference,
787 Clearwater, FL.
788 Liu, Y., Lu, K., Ma, Y., Yang, X., Zhang, W., Wu, Y., Peng, J., Shuai, S., Hu, M., Zhang, Y.,
789 (2017). Direct emission of nitrous acid (HONO) from gasoline cars in China determined by
790 vehicle chassis dynamometer experiments. *Atmos Environ.* 169: 89-96.
791 Liu, H., Ma, J., Dong, F., Yang, Y., Liu, X., Ma, G., Zheng, Z., Yao, M., (2018). Experimental
792 investigation of the effects of diesel fuel properties on combustion and emissions on a multi-
793 cylinder heavy-duty diesel engine. *Energy Convers Manage.* 171: 1787-1800.
794 Louis, C., Liu, Y., Tassel, P., Perret, P., Chaumond, A., André, M., (2016). PAH, BTEX,
795 carbonyl compound, black-carbon, NO2 and ultrafine particle dynamometer bench emissions
796 for Euro 4 and Euro 5 diesel and gasoline passenger cars. *Atmos Environ.* 141: 80-95.
797 Mayer, H., (1999). Air pollution in cities. *Atmos Environ.* 33: 4029-4037.
798 Miguel, A., Kirchstetter, T., Harley, R., Hering, S., (1998). On-road emissions of particulate
799 polycyclic aromatic hydrocarbons and black carbon from gasoline and diesel vehicles. *Environ*
800 *Sci Technol.* 32(4): 450-455.
801 Miller, J. and Bowman, C., (1989). Mechanism and modelling of nitrogen chemistry in
802 combustion. *Prog Energ Combust.* 15(4): 287-338.

803 Musculus, M.P.B., (2004). On the correlation between NO_x emissions and the diesel premixed
804 burn. *SAE J-Automot Eng*. 2004-01-1401.
805 Nakashima, Y. and Kajii, Y., (2017). Determination of nitrous acid emission factors from a
806 gasoline vehicle using a chassis dynamometer combined with incoherent broadband cavity-
807 enhanced absorption spectroscopy. *Sci Total Environ.* 575: 287-293.
808 Ning, Z., Polidori, A., Schauer, J., Sioutas, C., (2008). Emission factors of PM species based on
809 freeway measurements and comparison with tunnel and dynamometer studies. *Atmos Environ.*
810 42(13): 3099-3114.
811 Ning, Z., Wubulihairen, M., Yang, F., (2012). PM, NO_x and butane emissions from on-road
812 vehicle fleets in Hong Kong and their implications on emission control policy. *Atmos Environ.*
813 61: 265-274.
814 Pang, Y., Fuentes, M., Rieger, P., (2014). Trends in the emissions of Volatile Organic
815 Compounds (VOCs) from light-duty gasoline vehicles tested on chassis dynamometers in
816 Southern California. *Atmos Environ.* 83: 127-135.
817 Pope III, C.A., Burnett, R.T., Thun, M.J., Calle, E.E., Krewski, D., Ito, K., Thurston, G.D.,
818 (2002). Lung Cancer, Cardiopulmonary Mortality, and Long-term Exposure to Fine Particulate
819 Air Pollution. *JAMA-J Am Med Assoc.* 287(9): 1132-1141.

820 Rahman, S., Masjuki, H., Kalam, M., Abedin, M., Sanjid, A., Sajjad, H., (2013). Impact of idling
821 on fuel consumption and exhaust emissions and available idle-reduction technologies for diesel
822 vehicles – A review. *Energ Convers Manage.* 74: 171-182.
823 Rappengluck, B., Lubertino, G., Alvarez, S., Golovko, J., Czader, B., Ackermann, L., (2013).
824 Radical precursors and related species from traffic as observed and modeled at an urban
825 highway junction. *J. Air Waste Manag. Assoc.*, 63:11, 1270-1286.
826 Salvi, S., Blomberg, A., Rudell, B., Kelly, F., Sandstrom, T., Holgate, S., Frew, A., (1999). Acute
827 inflammatory responses in the airways and peripheral blood after short-term exposure to diesel
828 exhaust in healthy human volunteers. *Am J Resp Crit Care.* 159(3): 702-709.
829 Shah, S., Cocker, D., Miller, J. and Norbeck, J., (2004). Emission Rates of Particulate Matter and
830 Elemental and Organic Carbon from In-Use Diesel Engines. *Environ Sci Technol.* 38(9): 2544-
831 2550.
832 Sydbom, A., Blomberg, A., Parnia, S., Stenfors, N., Sandström, T., Dahlén, S., (2001). Health
833 effects of diesel exhaust emissions. *Eur Respir J.* 17(4): 733-746.
834 Tang, S., LaDuke, G., Whitby, R., Li, M. and Mazurek, M., (2008). Comparison of Regulated
835 and PM2.5 EC/OC Emissions from Light-Duty Gasoline, Diesel and CNG Vehicles over
836 Different Driving Cycles. *SAE Int. J. Fuels Lubr.* 1(1):1290-1306.
837 UNECE, (2011a). Consolidated Resolution on the Construction of Vehicles (R.E.3), Revision 2.
838 UNECE - United Nations Economic Commission for Europe, Geneva, Switzerland.

839 UNECE, (2011b). Regulation No. 83. Uniform provisions concerning the approval of vehicles
840 with regard to the emission of pollutants according to engine fuel requirements. In: Addendum
841 82: Regulation No. 83, Revision 4. UNECE - United Nations Economic Commission for
842 Europe, Geneva, Switzerland.
843 Wang, X., Westerdahl, D., Hu, J., Wu, Y., Yin, H., Pan, X., Max Zhang, K., (2012). On-road
844 diesel vehicle emission factors for nitrogen oxides and black carbon in two Chinese cities.
845 *Atmos Environ.* 46: 45-55.
846 Wang, L., Qu, F., Zhang, Y., Weschler, L., Sundell, J., (2015). Home environment in relation to
847 allergic rhinitis among preschool children in Beijing, China: A cross-sectional study. *Build*
848 *Environ.* 93: 54-63.
849 Weilenmann, M., Soltic, P., Saxer, C., Forss, A., Heeb, N., (2005). Regulated and nonregulated
850 diesel and gasoline cold start emissions at different temperatures. *Atmos Environ.* 39(13):
851 2433-2441.
852 Weiss, M., Bonnel, P., Hummel, R., Provenza, A., Manfredi, U., (2011). On-Road Emissions of
853 Light-Duty Vehicles in Europe. *Environ Sci Technol.* 45: 8575-8581.
854 Weiss, M., Bonnel, P., Kühlwein, J., Provenza, A., Lambrecht, U., Alessandrini, S., Carriero, M.,
855 Colombo, R., Forni, F., Lanappe, G., Le Lijour, P., Manfredi, U., Montigny, F., Sculati, M.,

856 (2012). Will Euro 6 reduce the NO_x emissions of new diesel cars? – Insights from on-road tests
857 with Portable Emissions Measurement Systems (PEMS). *Atmos Environ.* 62: 657-665.
858 Yanowitz, J., Graboski, M., Ryan, L., Alleman, T., McCormick, R., (1999). Chassis
859 dynamometer study of emissions from 21 in-use heavy-duty diesel vehicles. *Environ Sci*
860 *Technol.* 33(2): 209-216.
861 Yanowitz, J., McCormick, R., Graboski, M., (2000). In-use emissions from heavy-duty diesel
862 vehicles. *Environ Sci Technol.* 34(5): 729-740.
863 Yao, Z., Wu, B., Wu, Y., Cao, X., Jiang, X., (2015). Comparison of NO_x emissions from China
864 III and China IV in-use diesel trucks based on on-road measurements. *Atmos Environ.* 123: 1-8.
865 Yli-Tuomi, T., Aarnio, P., Pirjola, L., Mäkelä, T., Hillamo, R., Jantunen, M., (2005). Emissions
866 of fine particles, NO_x, and CO from on-road vehicles in Finland. *Atmos Environ.* 39(35): 6696-
867 6706.
868 Zare, A., Nabi, M. N., Bodisco, T. A., Hossain, F. M., Rahman, M. M., Chu Van, T., Ristovski, Z.
869 D., Brown, R. J., (2017). Diesel engine emissions with oxygenated fuels: A comparative study
870 into cold-start and hot-start operation. *J Clean Prod.* 162: 997-1008.
871 Zare, A., Bodisco, T. A., Nabi, M. N., Hossain, F. M., Ristovski, Z. D., Brown, R. J., (2018). A
872 comparative investigation into cold-start and hot-start operation of diesel engine performance
873 with oxygenated fuels during transient and steady-state operation. *Fuel.* 228: 390-404.

874 Zervas, E. and Bikas, G., (2008). Impact of the Driving Cycle on the NO_x and Particulate Matter
875 Exhaust Emissions of Diesel Passenger Cars. *Energ Fuel.* 22(3): 1707-1713.
876 Zheng, X., Zhang, S., Wu, Y., Zhang, K., Wu, X., Li, Z. and Hao, J., (2017). Characteristics of
877 black carbon emissions from in-use light-duty passenger vehicles. *Environ Pollut.* 231: 348-
878 356.

879 **Table 1.** Detailed information on tested diesel vehicles.

ID	Class	Weight (kg)	Testing Weight (kg)	Manufacturer	Model	First Registration	Transmission type	Emission standard	After treatment devices	Pre-test odometer (km)	Engine type	Engine capacity	Engine power
1	PC	2060	2405	Toyota	Grand Hiace	2002	4AT	EURO 3	/	337101	L4	2.982	75 kW / 3600 rpm
2	PC	2048	2485	Ssangyong	Stavic	2016	7AT	EURO 6	EGR[1], DPF[2], DOC[3]	5883	L4	2.157	131 kW / 4000 rpm
3	LDV	1590	2195	Toyota	Hiace	2000	5MT	EURO 2	/	440048	L4	3	100 kW / 3400 rpm
4	LDV	1730	2265	Toyota	Hiace	2005	5MT	EURO 3	EGR	147635	L4	2.494	75 kW / 3600 rpm
5	LDV	2080	2650	Hyundai	H-1	2008	5MT	EURO 4	EGR	195997	L4	2.497	125 kW / 3800 rpm
6	LDV	1910	2605	Nissan	Urvan	2008	5MT	EURO 4	EGR	98999	L4	2.953	78 kW / 3800 rpm
7	LDV	1570	2150	Toyota	Hiace	2015	AT	EURO 5	EGR, DPF	15836	L4	2.982	106 kW / 3400 rpm
8	MDV	3870	4685	Isuzu	NPR	2004	5MT	EURO 3	EGR	438083	L4	4.751	110 kW / 2600 rpm
9	MDV	4850	6900	Isuzu	NPR	2005	5MT	EURO 4	EGR	318360	L4	4.751	117 kW / 2900 rpm
10	MDV	4310	4900	Isuzu	NPR	2007	MT	EURO 4	EGR, DPF	234787	L4	5.193	114 kW / 2600 rpm
11	MDV	7073	11050	Mitsubishi	Fuso	2008	6MT	EURO 4	EGR, DPF, DOC	205702	L6	7.545	140 kW / 2900 rpm
12	MDV	5670	8035	UD	MKB	2009	6MT	EURO 4	EGR	220241	L6	7.684	182 kW / 2500 rpm
13	MDV	3967	4700	Isuzu	NPR	2010	MT	EURO 5	EGR, DPF	275356	L4	5.193	116 kW / 2600 rpm
14	HDV	17680	19000	Isuzu	CYH	2008	7MT	EURO 4	EGR, DOC	390829	L6	15.681	260 kW / 2000 rpm
15	HDV	9780	23000	Sinotruk	HOWO_A7	2012	16MT	EURO 5	SCR[4]	93232	L6	11.596	313 kW / 2200 rpm

880 *[1]EGR: Exhausted gas recirculation*

881 *[2]DPF: Diesel particulate filter*

882 *[3]DOC: Diesel oxidation catalysis*

883 *[4]SCR: Selective catalytic reduction*

884

885 **Table 2.** R^2 and p values of the linear regression of NO_x *EF* with different vehicle parameters under different driving cycles.

886

887 (a)

PC + LDV								
	Cold		Hot		Idle		Steady	
	R^2	**p-value**	**R^2**	**p-value**	**R^2**	**p-value**	**R^2**	**p-value**
Testing weight (kg)	0.20	0.3	0.30	0.2	/	/	0.16	0.4
Mileage (km)	0.13	0.4	0.079	0.5	0.00067	1	0.19	0.3
Maximum engine power (kW)	0.062	0.6	0.12	0.4	0.088	0.5	0.076	0.5

888

889 (b)

MDV + HDV								
	Cold		Hot		Idle		Steady	
	R^2	**p-value**	**R^2**	**p-value**	**R^2**	**p-value**	**R^2**	**p-value**
Testing weight	0.81*	<0.005*	0.67*	<0.05*	/	/	0.42	0.08
Mileage (km)	0.15	0.3	0.34	0.1	0.012	0.8	0.41	0.09
Maximum engine power (kW)	0.92*	<0.0005*	0.77*	<0.005*	0.25	0.2	0.48	0.06

Figure Captions

Fig. 1. Schematic diagram of the instrumental setup

Fig. 2. Speed vs. time trace of FIGE and NEDC cycles.

Fig. 3. *EF*s of CO, THC, NO_x and PM for 15 tested diesel vehicles in different driving cycles. The dashed lines in Fig.3 represent the average EFs of CO, THC, NOx, and PM over all driving cycles (i.e. cold-start, hot-start, idle, and steady-state) for each tested diesel vehicle.

Fig. 4. Emission ratios of (a) THC/NO_x and (b) CO/NO_x.

Fig. 5. Averaged *EF*s of THC, CO, NO_x and PM under different driving cycles.

Fig. 6. The cumulative average concentration of NO_x of (a) NEDC and (b) FIGE cycle.

Fig. 7. Average *EF*s of NO_x and PM of all vehicles. Numbers in Fig. 6(a) represent the corresponding vehicle ID of the data point. Black dashed lines correspond to Euro 3 standard for MDV. Fig. 6(b) is the enlargement of the black squared area of Fig. 6(a).

Fig. 8. Correlation between NO_x *EF*s and (a) testing weight in cold-start and (b) hot-start, as well as (c) maximum engine power in cold-start and (d) hot-start condition.

904

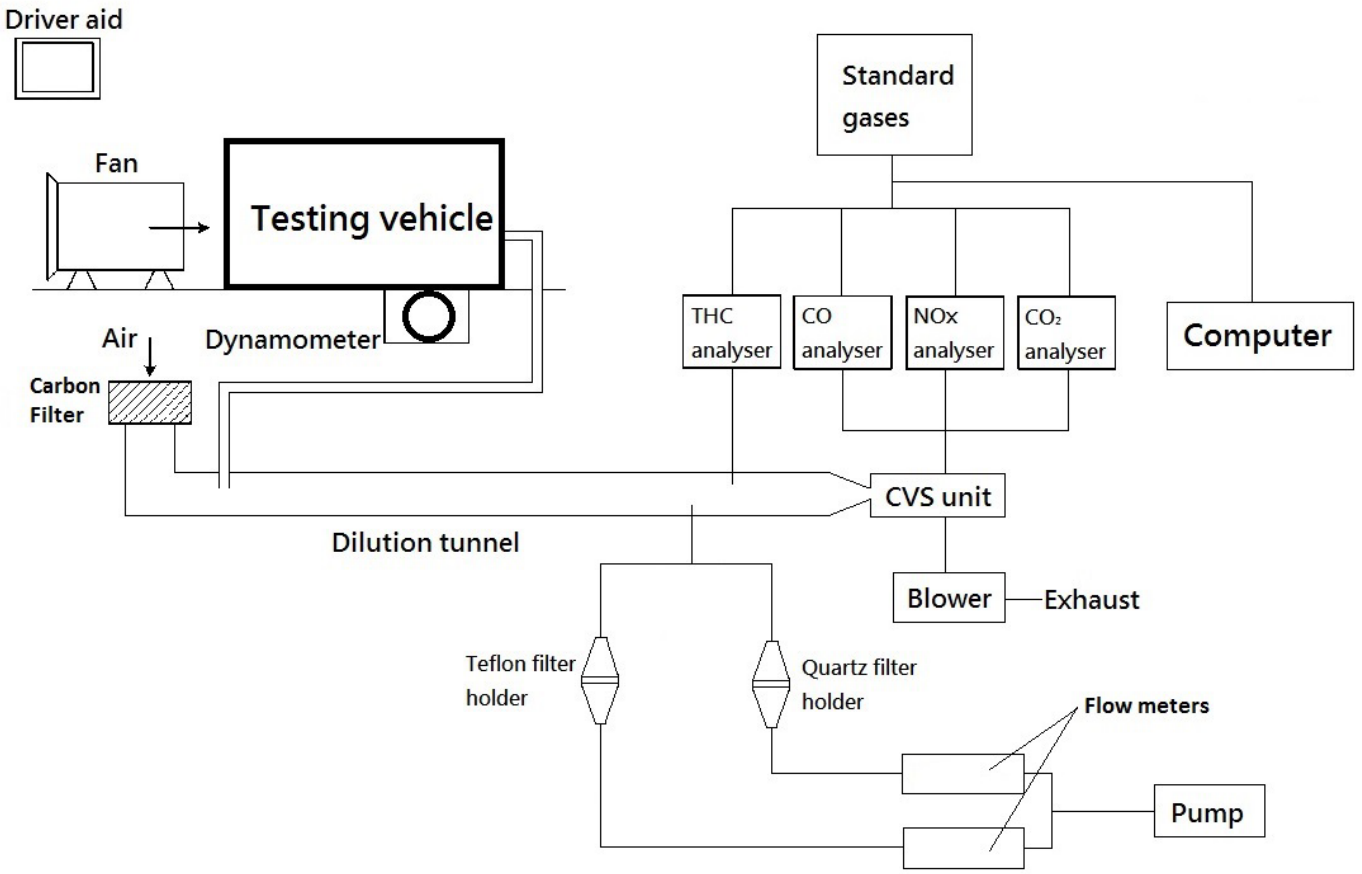

905

906 **Fig. 1.**

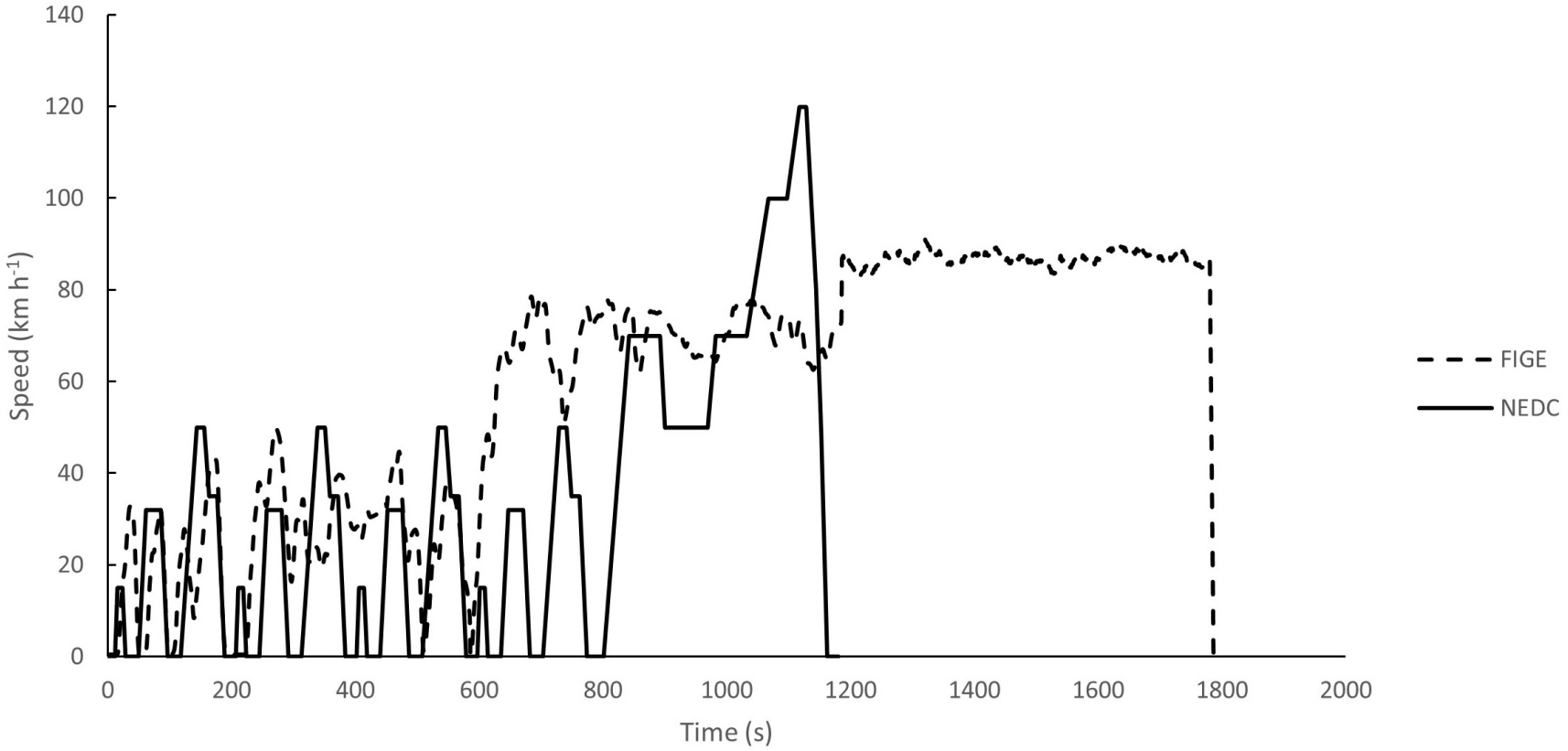

907

908 **Fig. 2.**

909

910

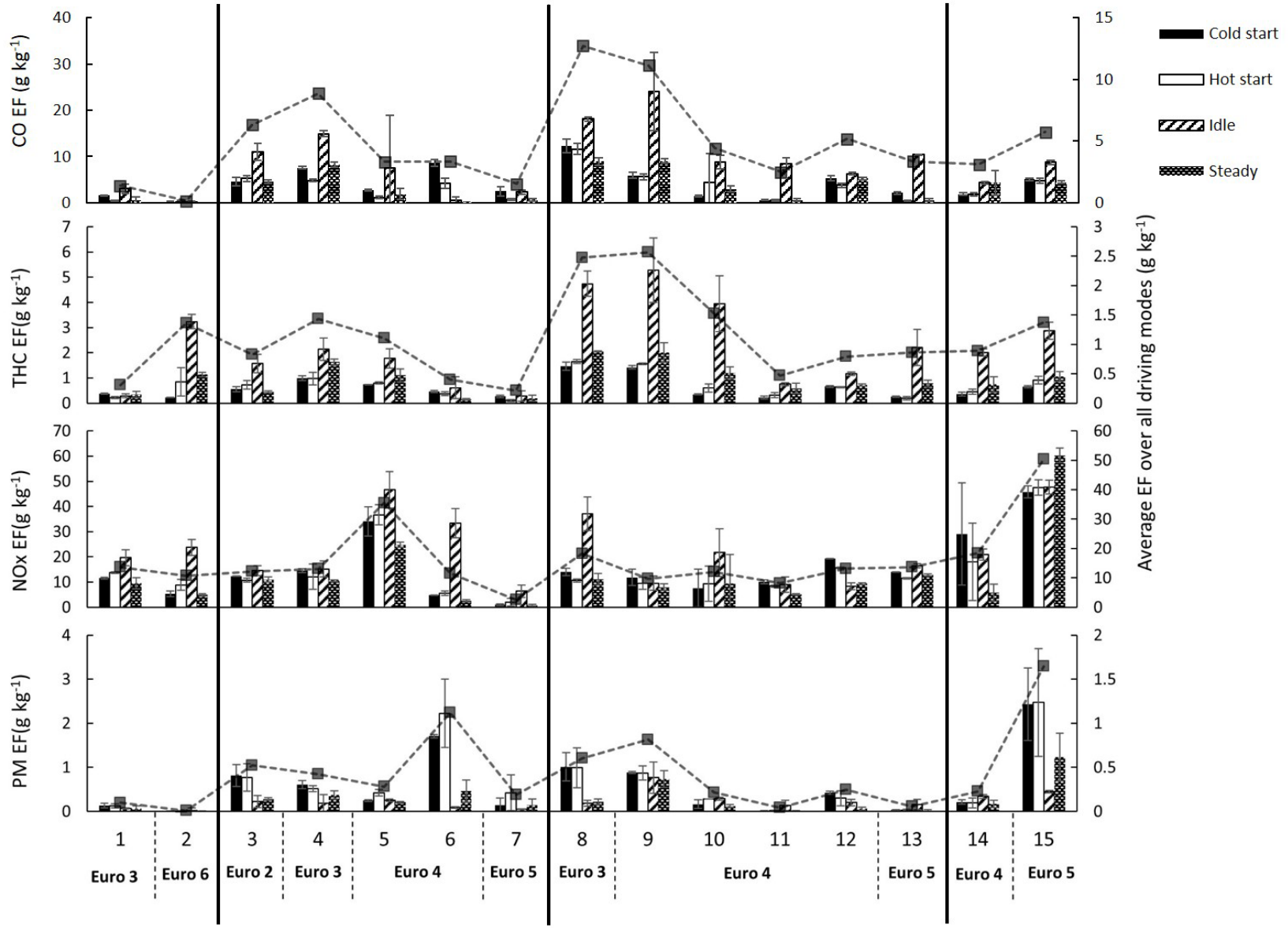
CO EF (g kg-1)
THC EF(g kg-1)
NOx EF(g kg-1)
PM EF(g kg-1)
Average EF over all driving modes (g kg-1)
Cold start
Hot start
Idle
Steady
1 2 3 4 5 6 7 8 9 10 11 12 13 14 15
Euro 3 Euro 6 Euro 2 Euro 3 Euro 4 Euro 5 Euro 3 Euro 4 Euro 5 Euro 4 Euro 5

911

Fig. 3.

912 (a)

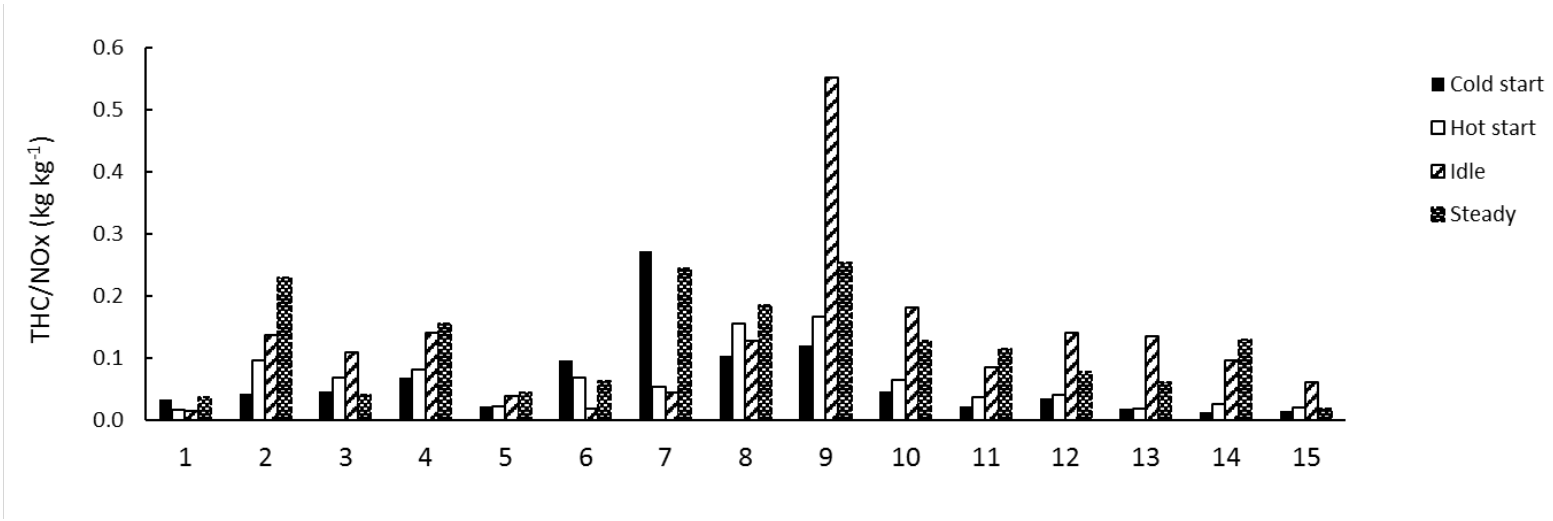

913 (b)

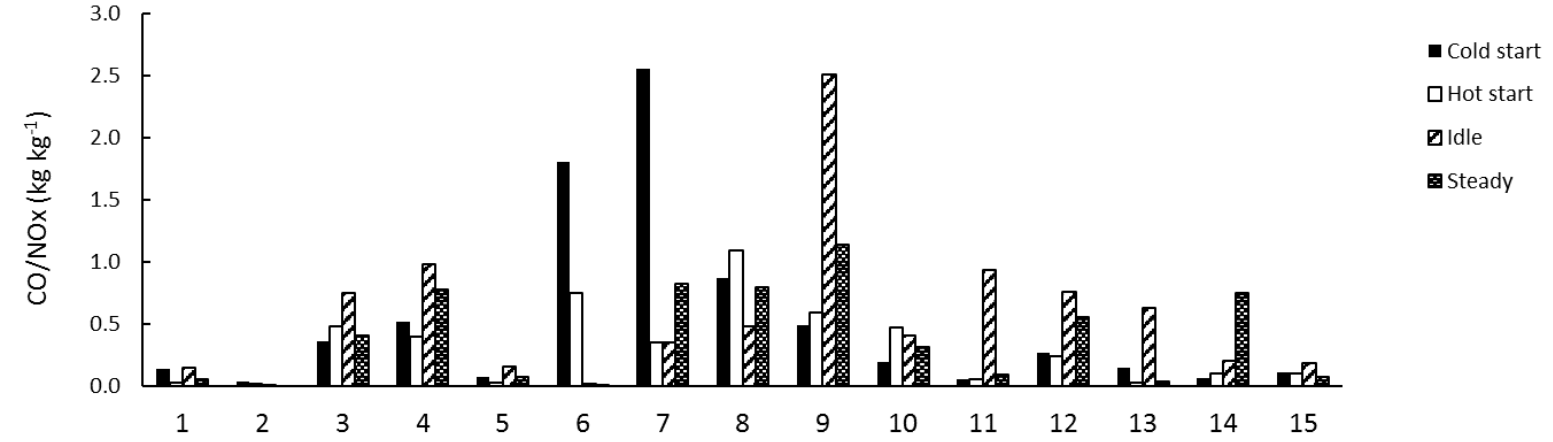

914 **Fig. 4.**

915

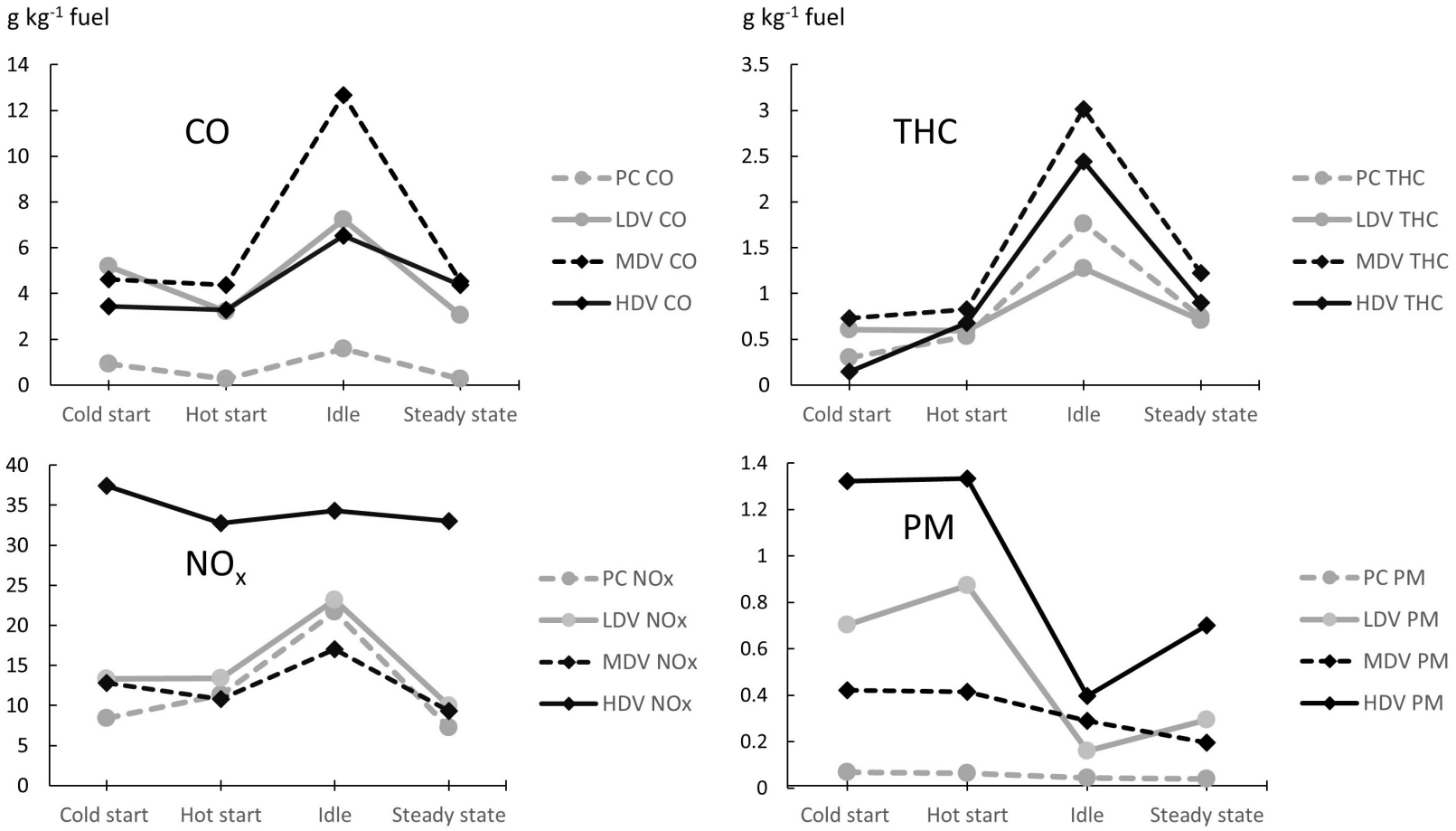

916

917 **Fig. 5.**

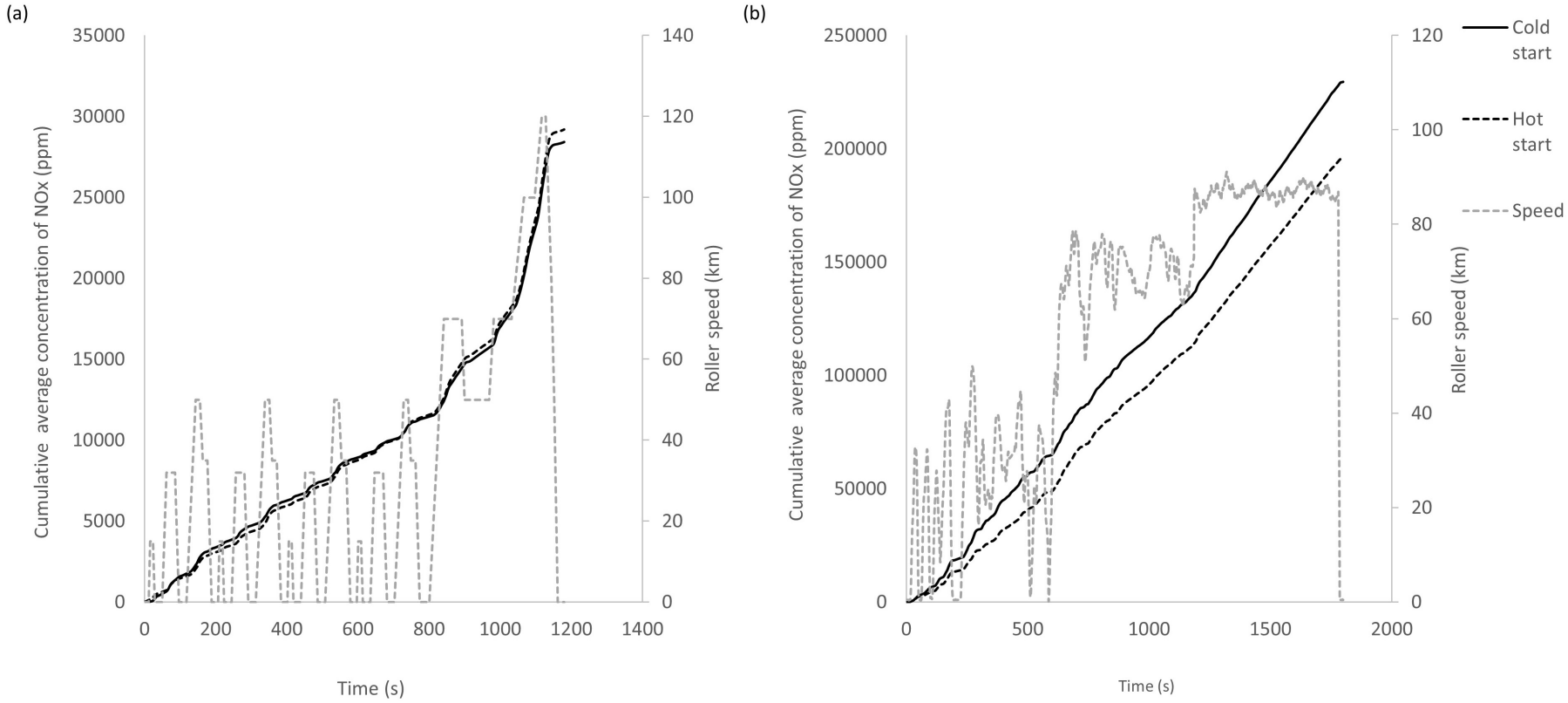
(a)
Cumulative average concentration of NOx (ppm)
Roller speed (km)
Time (s)
0
5000
10000
15000
20000
25000
30000
35000
0
20
40
60
80
100
120
140
0
200
400
600
800
1000
1200
1400
(b)
Cumulative average concentration of NOx (ppm)
Roller speed (km)
Time (s)
0
50000
100000
150000
200000
250000
0
20
40
60
80
100
120
0
500
1000
1500
2000
Cold start
Hot start
Speed

Fig. 6.

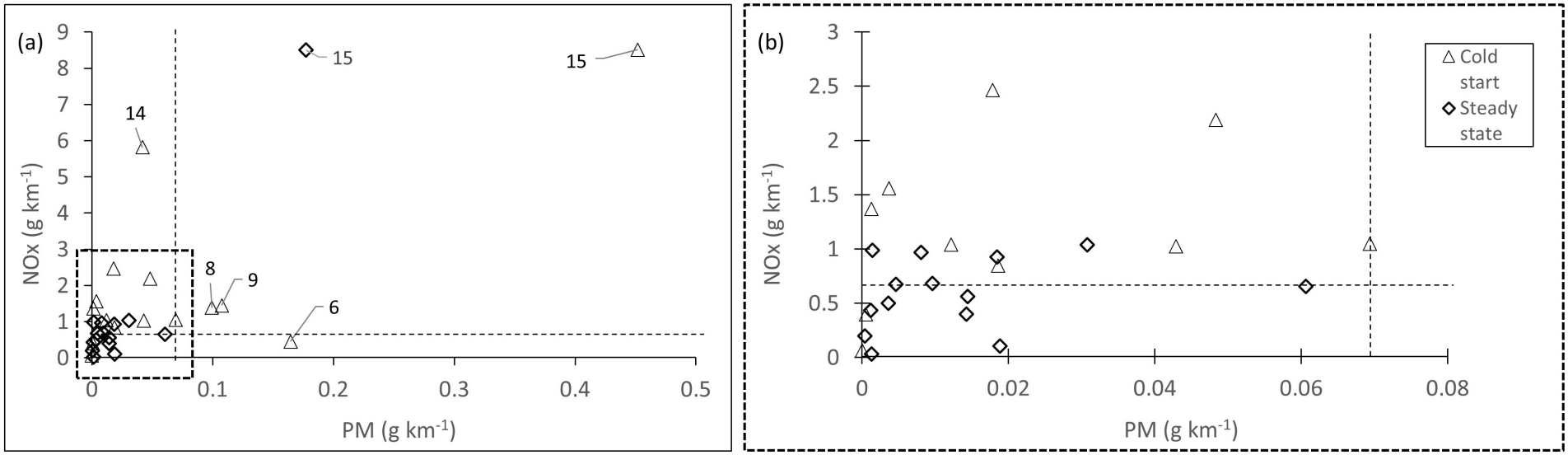

921

922 **Fig. 7.**

923

924

925

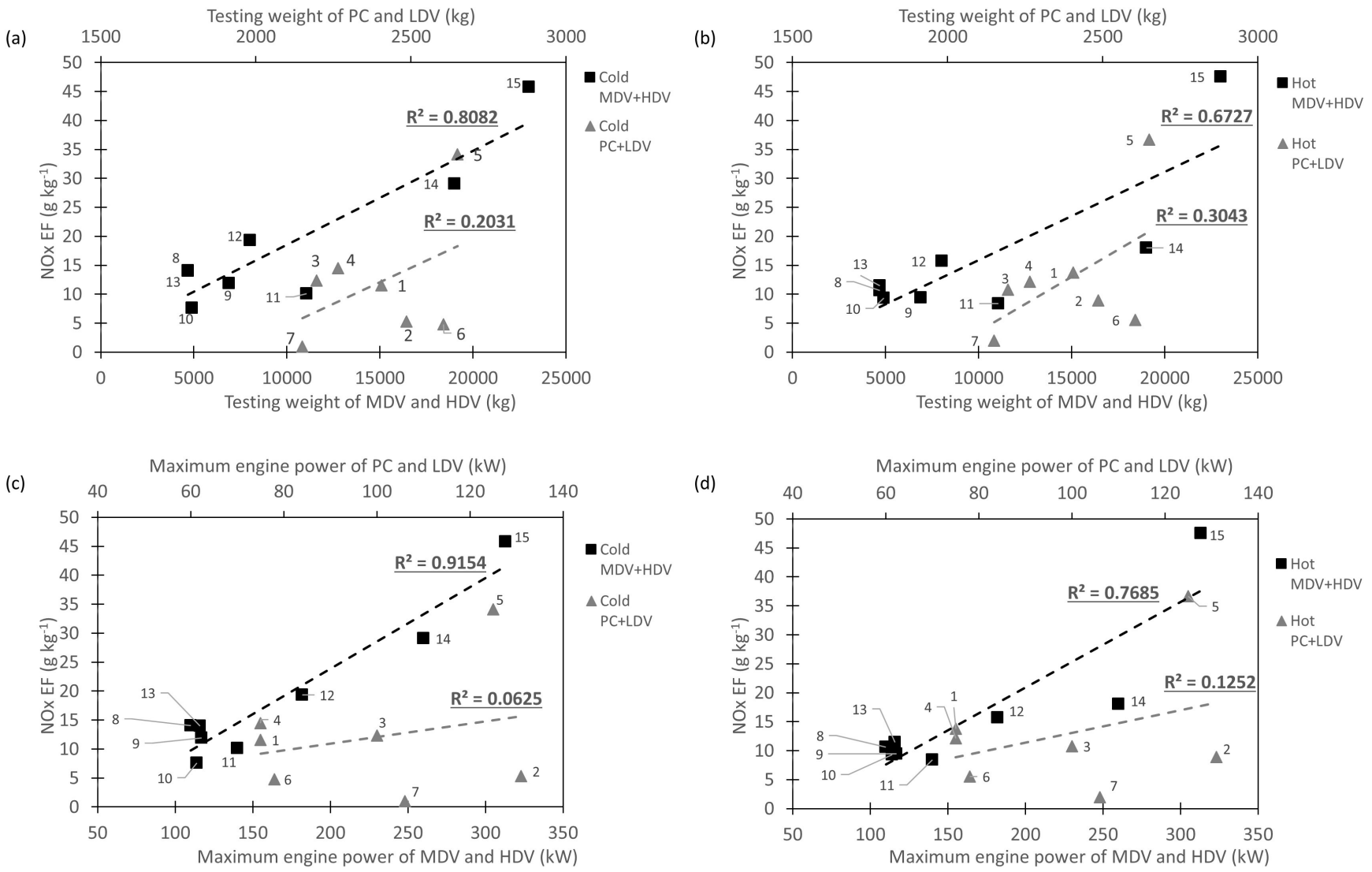
(a)
Testing weight of PC and LDV (kg)
1500
2000
2500
3000
NOx EF (g kg-1)
Testing weight of MDV and HDV (kg)
0
5000
10000
15000
20000
25000
R² = 0.8082
R² = 0.2031
Cold MDV+HDV
Cold PC+LDV
(b)
R² = 0.6727
R² = 0.3043
Hot MDV+HDV
Hot PC+LDV
(c)
Maximum engine power of PC and LDV (kW)
40
60
80
100
120
140
Maximum engine power of MDV and HDV (kW)
50
100
150
200
250
300
350
R² = 0.9154
R² = 0.0625
(d)
R² = 0.7685
R² = 0.1252

926

927 **Fig. 8.**